Spring 2015

Design and heat transfer analysis of accelerating distributed combustion system

Yashovardhan U. Wagh
Purdue University

Graduate School Form 30
Updated 1/15/2015

PURDUE UNIVERSITY
GRADUATE SCHOOL
Thesis/Dissertation Acceptance

This is to certify that the thesis/dissertation prepared

By Yashovardhan U Wagh

Entitled
DESIGN AND HEAT TRANSFER ANALYSIS OF ACCELERATING DISTRIBUTED COMBUSTION SYSTEM

For the degree of Master of Science in Mechanical Engineering

Is approved by the final examining committee:

Dr. Robert Lucht
Chair

Dr. Hukam Mongia

Dr. Sameer Naik

To the best of my knowledge and as understood by the student in the Thesis/Dissertation Agreement, Publication Delay, and Certification Disclaimer (Graduate School Form 32), this thesis/dissertation adheres to the provisions of Purdue University's "Policy of Integrity in Research" and the use of copyright material.

Approved by Major Professor(s): Dr. Robert Lucht

Approved by: Dr. Ganesh Subbarayan 4/10/2015

Head of the Departmental Graduate Program Date

DESIGN AND HEAT TRANSFER ANALYSIS OF ACCELERATING DISTRIBUTED COMBUSTION SYSTEM

A Thesis

Submitted to the Faculty

of

Purdue University

by

Yashovardhan U. Wagh

In Partial Fulfillment of the

Requirements for the Degree

of

Master of Science in Mechanical Engineering

May 2015

Purdue University

West Lafayette, Indiana

Dedicated to my mother, Varsha, for without her support, encouragement, and sacrifices I would not have achieved anything. A special thanks and undying gratitude to my advisors Dr. Robert Lucht and Dr. Sameer Naik for guiding me in the right direction at every step of my Purdue life.

ACKNOWLEDGEMENTS

I would like to thank Dr. Lucht for giving me an opportunity to work under his guidance and for providing financial support. I also thank Dr. Naik and Dr. Mongia for their encouragement and help.

This entire work has been done in collaboration with Pratikash Panda and his guidance and help have been exemplary. I would like to thank Mario Roa, Scott Meyer, and the entire Gas Turbine Combustion Facility research team at Zucrow Laboratories for their inputs and help. I would also like to acknowledge the role of all machinists at various places who have helped us manufacture and put together our rig in a timely fashion.

I would like to thank my friends Joey, Riaz, Karthik, Tom, Matt, Sagar, Shardul and Purval for all the wonderful experiences at Purdue. Last but not the least I would like to thank Anchalika who has motivated me in my work and been with me throughout my time at Purdue.

This research program was funded by Siemens Power Generation and was ably managed by Walter R. Laster.

TABLE OF CONTENTS

Page

Page

LIST OF TABLES

Table Page

LIST OF FIGURES

Figure Page

ABSTRACT

Wagh, Yashovardhan U. M.S.M.E., Purdue University, May 2015. Design and Heat Transfer Analysis of Accelerating Distributed Combustion System. Major Professor: Dr. Robert Lucht, School of Mechanical Engineering.

Over the past few decades, there has been a significant increase in greenhouse gases such as CO_2, N_2O, and CH_4 produced from gas turbine engines. Keeping this in mind, current research work is being carried out for reducing NOx produced from combustors. The objective of this research is to determine the feasibility of Distributed Combustion Systems (DCS) for increasing efficiency and reducing NOx emissions.

A DCS has a main combustion zone (MCZ) where 90% of the fuel is burned and is followed by a secondary combustion zone (SCZ) in which jets carrying fuel are injected into the vitiated crossflow from the MCZ. This fuel jet auto-ignites under the influence of the high temperature vitiated crossflow. A new type of accelerating distributed combustion system has been designed in this project. In the current design, higher Mach numbers of the main flow can be obtained at the jet exit after reducing the exit area of secondary combustion zone by about five times compared to the inlet. Along with the design, a detailed one-dimensional heat transfer analysis has been performed. A Matlab code was used to determine whether final temperatures of the thermal barrier coating (TBC)

and cooling water fall within acceptable design constraints. Conduction, convection, and radiation at steady state were used for determining heat transfer relationships between different materials. Water and nitrogen flow rates as well as the dimensions of cooling water channels were varied parametrically to find ideal conditions. Based on the heat transfer calculations, 8.5 gpm water are needed to cool the secondary combustion zone to maintain temperature within material property limits.

Various laser-based measurement techniques such as Planar Laser-Induced Flourescence (PLIF), Particle Image Velocimetry (PIV), and Coherent Anti-Stokes Raman Spectroscopy (CARS) will be performed to study the combustion in the accelerating flow channel. Emissions sampling will be performed downstream of combustion zone using a water-cooled sampling probe. These measurements will provide insight into the various physical phenomena associated with NOx production.

CHAPTER 1. INTRODUCTION

1.1 Motivation

The Third National Climate Assessment report [1] details how climate change impacts the United States and the rest of the world. There is evidence and theory which projects a temperature change of 5^{o}F over the next century. This temperature change is likely to have disastrous effects such as melting of glaciers, global weather changes, extreme precipitation variations, changes in sea levels, and decrease in natural flora and fauna.

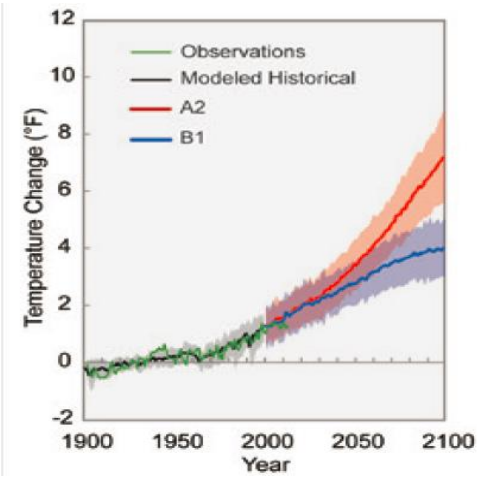

Figure 1.1: Projected Global Temperature Change [1].

In Fig 1.1, the lines represent a central estimate of global average temperature rise. Model A2 assumes continued increase in emissions whereas the model B1 assumes significant reduction in emissions. These temperature changes have been mainly

associated with increase in atmospheric concentration of greenhouse gases such as CO_2, N_2O, and CH_4. Concentration of nitrous oxide has increased approximately by 20% [1] compared to the pre-industrial era. Figure 1.2 below shows the increasing levels of heat trapping gases like carbon dioxide, methane, and nitrous oxide over the last 2000 years.

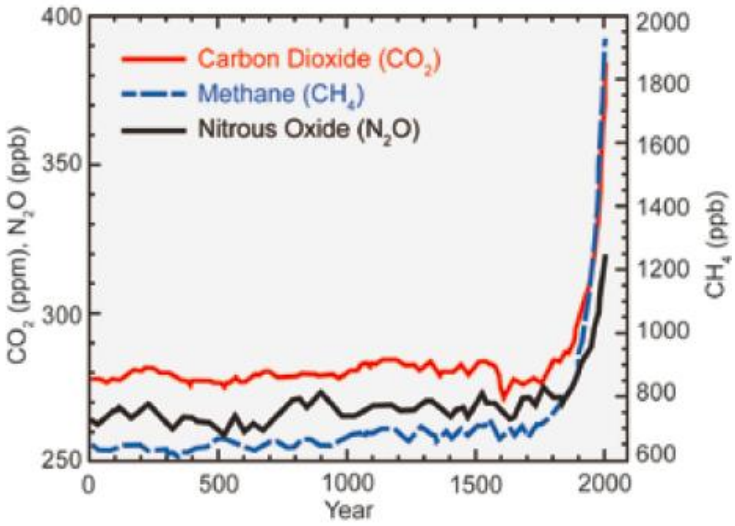

Figure 1.2: 2000 Years of Heat-Trapping Gas Levels [1].

One of the major sources contributing to increase in greenhouse gases is burning of fossil fuels. Power generation using fossil fuels serves as a major chunk of the energy pie of developing countries as well as industrially developed nations. In order to reduce dependence on traditional fuels, many countries are moving towards natural-gas-powered turbines due to their low installation costs along with shorter construction times. Many companies are conducting research to reduce NOx levels in combustors operating with natural gas.

1.2 Objective

The primary objective of this thesis is to provide critical information for successful manufacturing of an accelerating distributed combustion system. Following are the specific objectives of this work:

(a) To conceptualize the initial design considering the effect of combustor geometry on Mach number variations of the gases flowing through it. The length of combustor determines the angles of contraction and expansion for gases.

(b) To make the design compatible with the current rig at the Gas Turbine Combustion Facility at Zucrow. The new design must consider flow constraints for fuel, air, and cooling water.

(c) To perform heat transfer analysis using one-dimensional heat transfer model to determine appropriate cooling for the rig. Material constraints and properties for stainless steel, thermal barrier coating, and water have to be considered.

1.3 Overview

Chapter 2 includes a summary of prior research related to distributed combustion systems and previous work regarding the use of staged combustion systems to improve thermal efficiency by increasing the temperature. Recent research in constant area distributed combustion system and initial conceptualization of the proposed accelerated combustion system are discussed.

Chapter 3 presents the design of the experimental system including design specifications and detailed aspects related to the main combustion zone, secondary combustion zone, optical windows, water cooling channels, and other instrumentation.

Chapter 3 also describes a one-dimensional heat transfer analysis of the main combustion zone and secondary combustion zone in order to test the longevity and survival of the experimental rig.

Chapter 4 lists immediate future planned work using laser diagnostic techniques in the proposed new design. Also, changes in nozzle position which can enable visualization of jet in cross flow at different Mach numbers has been proposed for further in-depth studies.

CHAPTER 2. LITERATURE REVIEW

2.1 Distributed Combustion System (DCS)

In 1970s, NASA's Experimental Clean Combustor Program (ECCP) [2] proposed a staged combustion or distributed combustion system as an effective technology for reducing NOx emissions. Since then, secondary injection of fuel is being investigated by many gas turbine manufacturers and power generation companies as an effective way of reducing NOx emissions and simultaneously increasing the efficiency and power output of the engines. Figure 2.1 shows two staged combustion engines, viz. General Electric (GE) LM2500 and International Aero Engines (IAE) V2500 [3, 4].

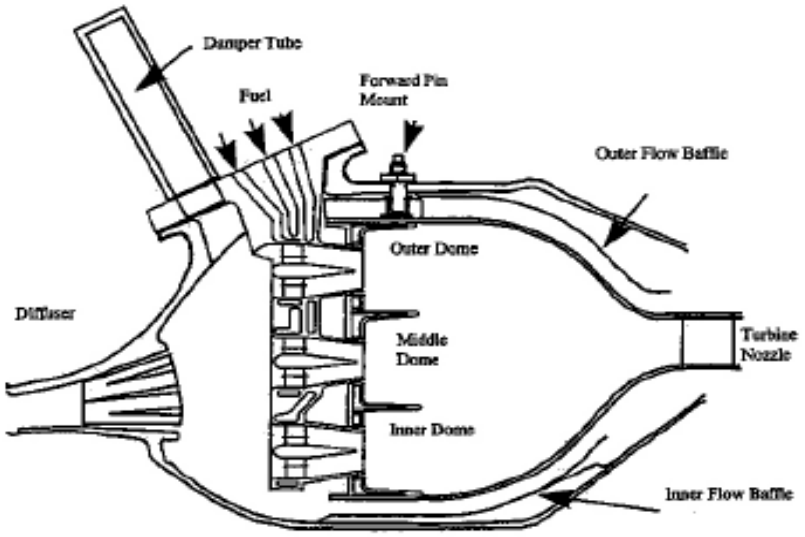

(a) GE LM2500

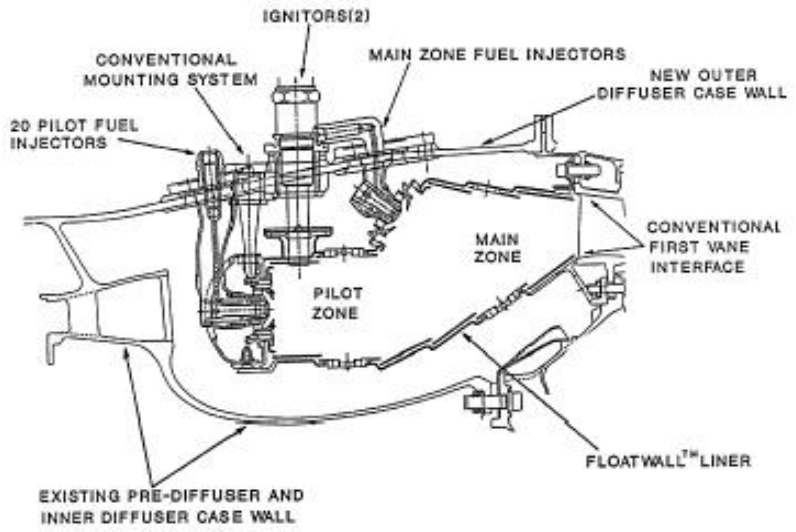

(b) IAE V2500

Figure 2.1: Cross Section views of two first-generation DCS [3, 4].

The main combustion zone, labelled as the pilot zone, in Fig. 2.1(b) provides rise in temperature needed for idle conditions. Eventually as the engine power increases, the main combustion zone acts like a pilot providing heat to aid rapid combustion in the secondary combustion zone, labelled as the main zone, in Fig 2.1(b).

2.2 Constant Area DCS

A constant area distributed combustion system was designed, fabricated, and studied over the last six years [5, 6]. A variety of measurements such as emission sampling, CH* chemiluminescense, particle image velocimetry, OH planar laser induced fluorescence and dual-pump coherent anti-Stokes Raman scattering have been performed. A schematic of this system is shown in Fig 2.2.

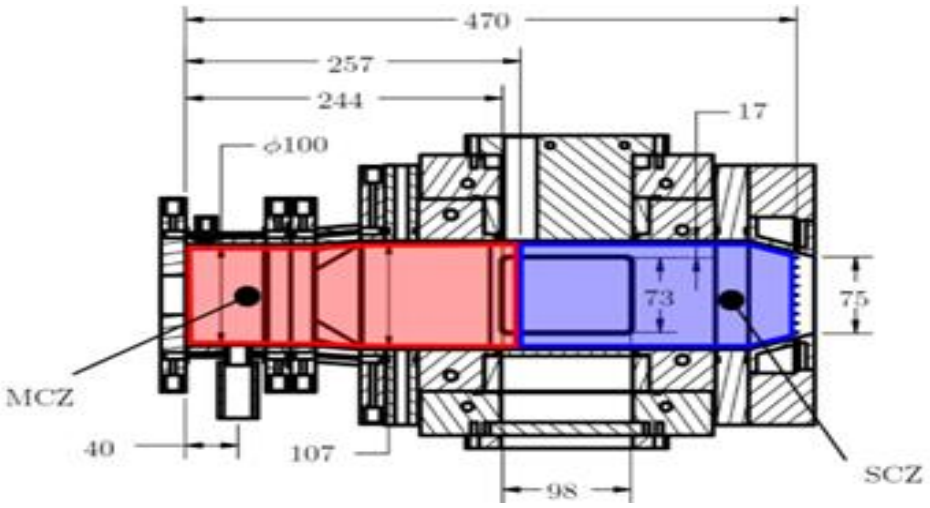

Figure 2.2: Cross-sectional view of constant area DCS at Purdue [5, 6].

One of the major outcomes from the constant area distributed combustion system experimentation was the demonstration of sub-10ppm NOx levels despite an increase in the exit temperature of combustion gases. The reduction in NOx formation is a result of the decrease in residence time at high temperature and the reduction in oxygen content.

2.3 Accelerating DCS

An accelerating passage secondary combustion zone has the potential to decrease NOx emissions further with additional decrease in residence time while maintaining high gas temperatures essential for higher engine efficiencies. With the accelerating DCS, an increase in the flow Mach number of gases combusting in the secondary combustion zone is expected. A decrease in static temperature of the flow results by increasing the gas flow velocity. Both these factors are favorable for NOx reduction. However, complete chemical reaction of injected fuel in the secondary combustion zone is also critical for decreasing fuel consumption and unburned hydrocarbons. Figure 2.3 shows that NOx levels

produced from Accelerating Swirl Passage (ASP) flame holders are nearly an order of magnitude lower compared to conventional lean direct injection (LDI) combustors and other high-speed research program combustors [7].

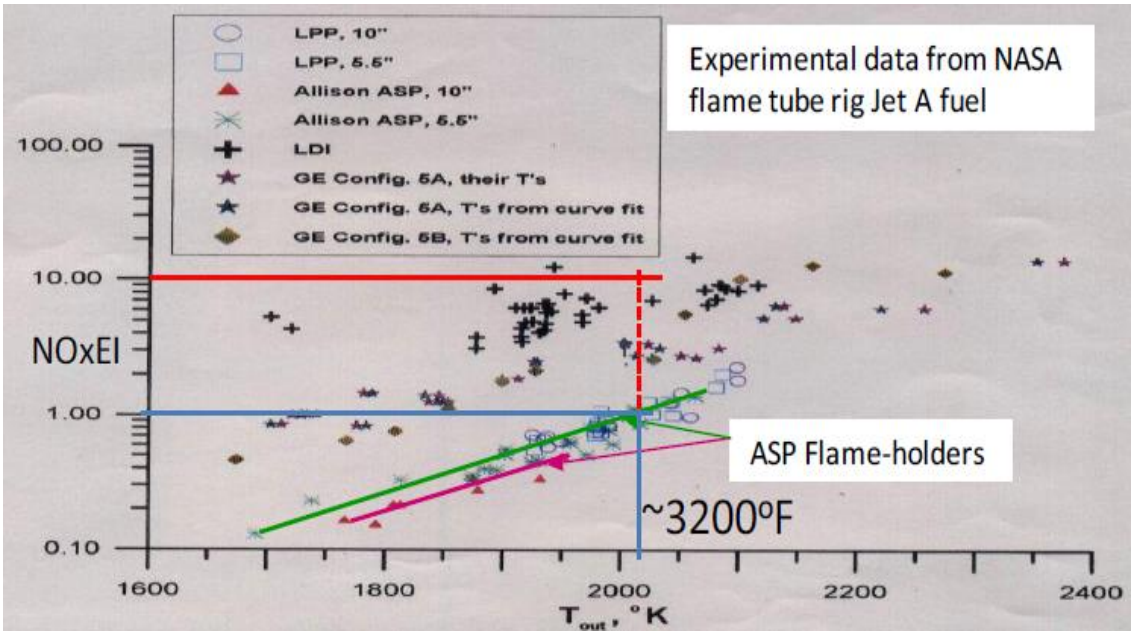

Figure 2.3: Comparison of NOx levels from ASP flame holders with other LDI and GEA HSR combustors [7].

CHAPTER 3. DESIGN AND HEAT TRANSFER ANALYSIS

3.1 Existing Constant Area DCS

The existing constant area DCS has an optical viewing area of 7742 mm^2 with window dimensions of 101.6 mm × 76.2 mm. Figure 3.1 shows a schematic diagram of the existing test rig [8].

Dividing the current design section by section for further understanding:

(a) Section 1.0 provides the inlet for heated air along with fuel from a fuel peg. The fuel peg has four 1.3 mm diameter holes. The holes are arranged such that two point towards the heated air and the other two are perpendicular to them. Four cylindrical bluff bodies are welded in series downstream of the fuel peg in order to ensure fuel and air mixing.

(b) Section 2.0 has a low swirl burner consisting of 16 axial vanes at an angle of 45^o and a series of small holes in the center. The burner has a swirl number of 0.5.

(c) Section 3.0 is the main combustion zone (MCZ) where the premixed flow enters the head end of the combustor having a diameter of 100 mm. Here the mixture is ignited and burned.

(d) Section 4.0 is the region in which flow cross-section changes from circular to square

(e) Sections 5.0 and 5.5 are the secondary combustion zone (SCZ), where secondary fuel is injected and reacting jet flow studies are performed using laser diagnostics since optical windows allow laser access.

(f) Section 6.0 is the combustion reaction quenching area where water at 1 gpm is injected to freeze NOx formation and destruction reactions.

(g) Section 7.0 is the region in which flow cross-section changes from square to circular.

(h) Section 8.0 allows uniform mixing of exhaust gases and emissions sampling is performed at the downstream end with the help of a water cooled probe.

(i) Section 9.0 enables further cooling of gases below 700 K before being exhausted into the atmosphere.

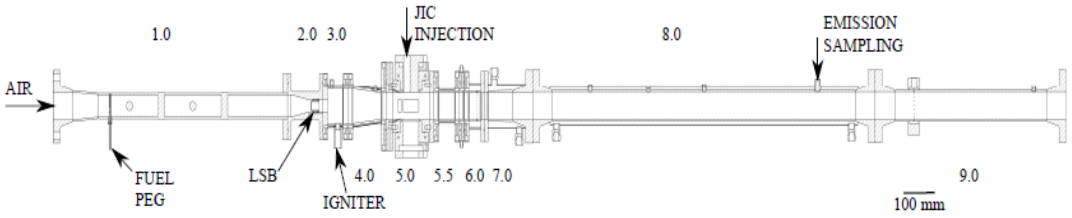

Figure 3.1: Overview of existing experimental rig [8].

3.2 Design

Figure 3.2 shows an overall schematic diagram of the proposed accelerating DCS. The incoming flow to the MCZ is composed of natural gas and air pressurized to 5.5 atm and maintained at an equivalence ratio of 0.5. The air entering the MCZ is heated to a temperature of 723 K and the flow rate will vary between 0.8 kg/s to 2.0 kg/s depending on the flow Mach number to be tested.

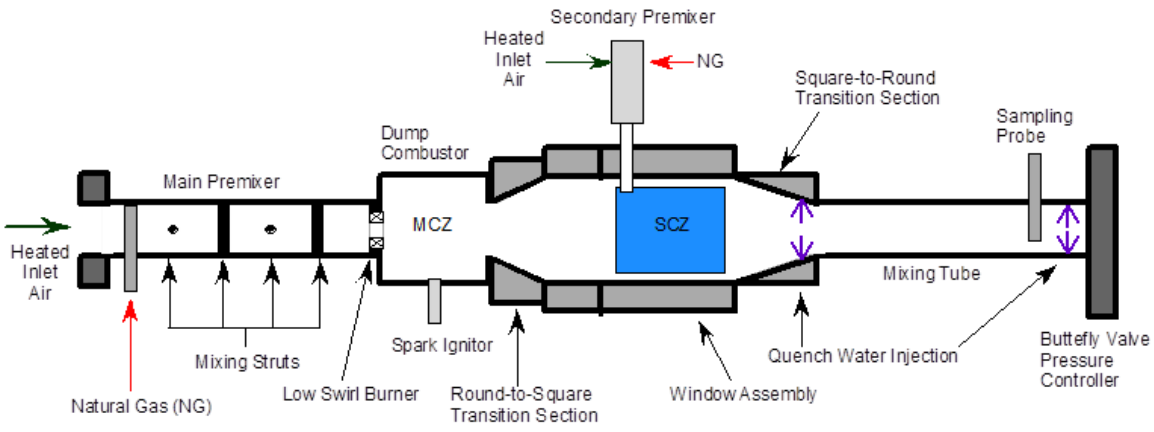

Figure 3.2: Overall schematic of proposed accelerating DCS.

Some of the operating conditions used for the rig are listed in Table 3.1

Table 3.1: Operating conditions for accelerating DCS.

Operating Pressure (atm)	5.5
Operating Temperature (K)	723
MCZ Air Flow Rate Range (kg/s)	0.8 – 2.0
MCZ Equivalence Ratio, ϕ_{main} = 0.5	0.5

3.2.1 Mach Number Calculations and Variations

A converging length of 10” followed by a straight section of 2” is chosen for the accelerating passage window combustor. We can visualize jets injected from the proposed location of the nozzle into the main flow at a Mach number of 0.3. Figure 3.3 shows the variation of Mach number for various convergence angles (θ). It is critical to note here the steep increase in Mach number towards the downstream end of the combustor, due to which a convergence angle Θ = 17.35^{o} and converging length of 10” is

chosen so that it easily matches the existing rig length and also enables visualization at different Mach numbers.

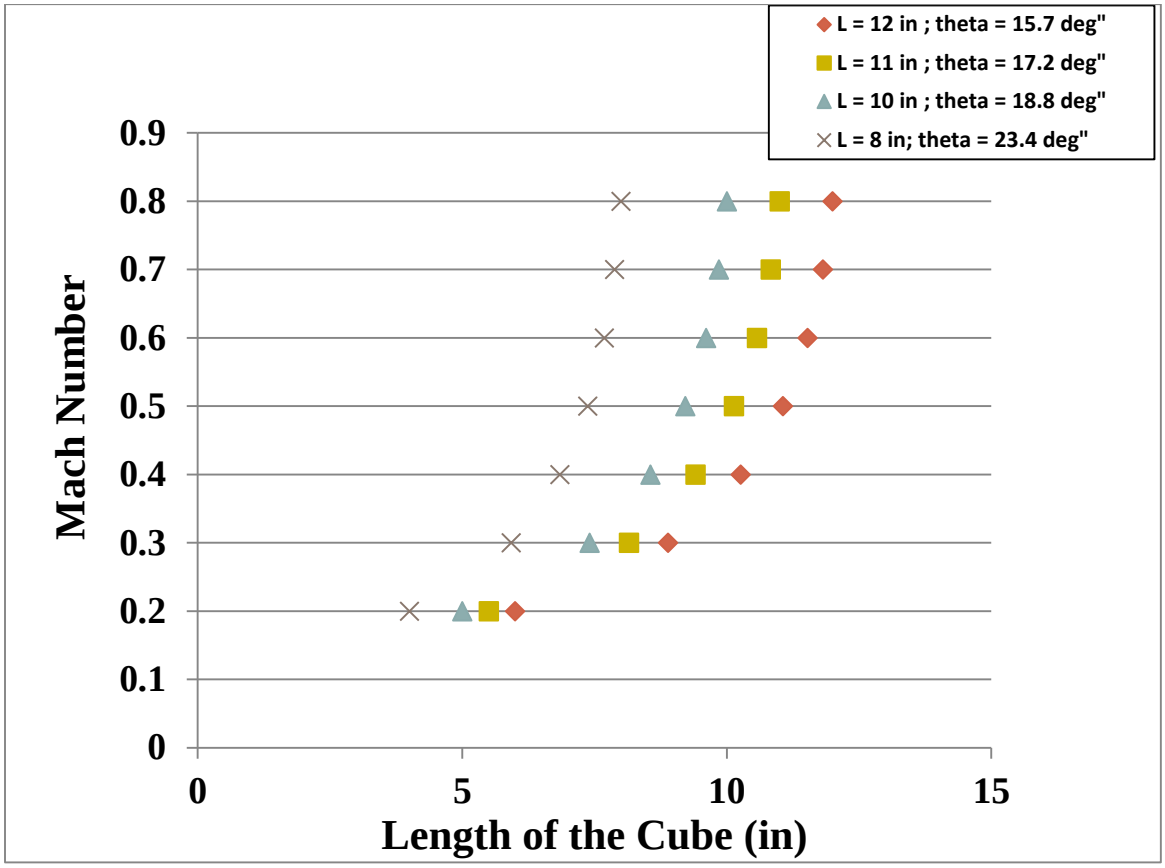

Figure 3.3: Variation of Mach number as a function of cube length for various convergence angles.

3.2.2 Area Calculations

Table 3.2 shows area calculations corresponding to increasing Mach numbers. These were performed to determine the exit area of the accelerating flow chamber. It was critical to maintain exit area such that the exit velocity is below sonic levels and at the same time maintain machinability for fabricating the combustor.

Table 3.2: Exit area and length calculations corresponding to different Mach numbers.

Mach Number	Exit Area (in^2)	Exit Contracting Side (in)
0.113	17.6	4.2
0.2	10.67	2.5
0.3	7.32	1.7
0.4	5.71	1.4
0.5	4.8	1.1
0.6	4.25	1.0
0.7	3.91	0.9
0.8	3.7	0.880

3.2.3 Design and Material Specifications

The test rig is subjected to high temperatures, in the range of 700 K to 1150 K. Along with high temperatures, the rig also undergoes high pressure operation. Considering cost effectiveness and machinability, Stainless Steel 347 was chosen as the material for the manufacturing of accelerating distributed combustion system.

3.2.3.1 Film Cooling Louvre Design

A special film cooling louvre has been designed to equally distribute nitrogen, thus giving it appropriate momentum and direction. Nitrogen flows parallel to the optical windows, providing them with requisite cooling in order to avoid thermal stresses and also contributes towards maintaining appropriate mass flow rates. In Fig. 3.4, the arrow points towards the end of the louvre from where heated nitrogen will flow.

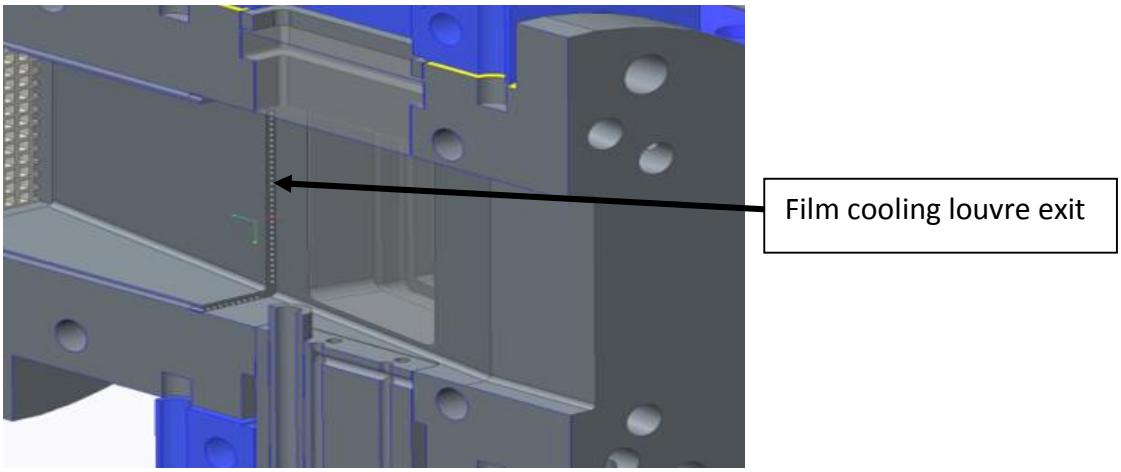

Figure 3.4: Film cooling louvre design for accelerating DCS.

3.2.3.2 Windows Configuration

The windows are aligned such that the distance between nozzle and opposing wall remains constant thus keeping the window opposite the nozzle parallel to it. The other two windows are at a gradient as seen in Fig. 3.6. All windows are double paned: the inner window experiences thermal load whereas the outer window experiences pressure load. Beam deflection angles were calculated using software TracePro and the results are tabulated in Table 3.3. The beam deflects towards the normal by a relatively small distance compared to the cavity dimensions, and should not cause any significant loss of viewing area.

Table 3.3: Deflection angles for 283 nm and 532 nm laser beams.

Beam Wavelength	Deflection Angle
283 nm	6.3^{o}
532 nm	6.4^{o}

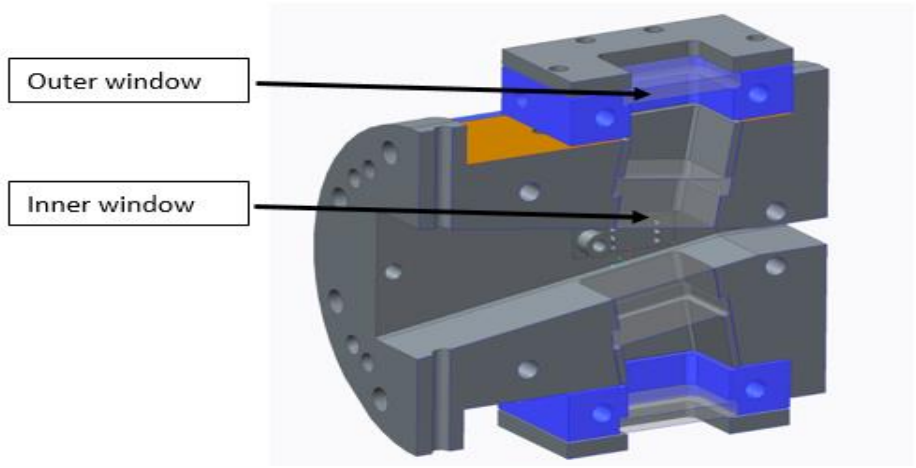

Figure 3.5: Window location in the accelerating DCS.

3.2.3.3 Nozzle Location

The proposed nozzle is at a distance of six inches from the inlet of the secondary combustion zone, enabling visualization of secondary fuel jet at Mach number of 0.3 for the main flow. Fig. 3.5 shows the proposed location of the nozzle with respect to the optical windows. The design allows various kinds of nozzles such as flush mounted or extended nozzles to be used during experimentation.

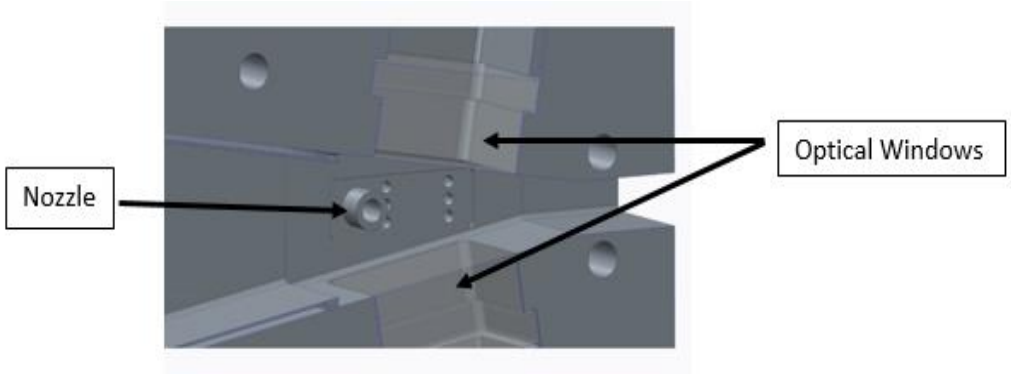

Figure 3.6: Location of nozzle with respect to optical windows in accelerating DCS.

3.2.3.4 Thermocouple Location

Thermocouples are located downstream of the nozzle as seen in Fig 3.7. The distance between the thermocouple tip and the combustion cavity is 5 mm; thus enabling accurate temperature measurements. They will be used for monitoring the temperatures near the throat where highest temperatures occur and for acquiring temperature data required for calculating heat loss from the rig.

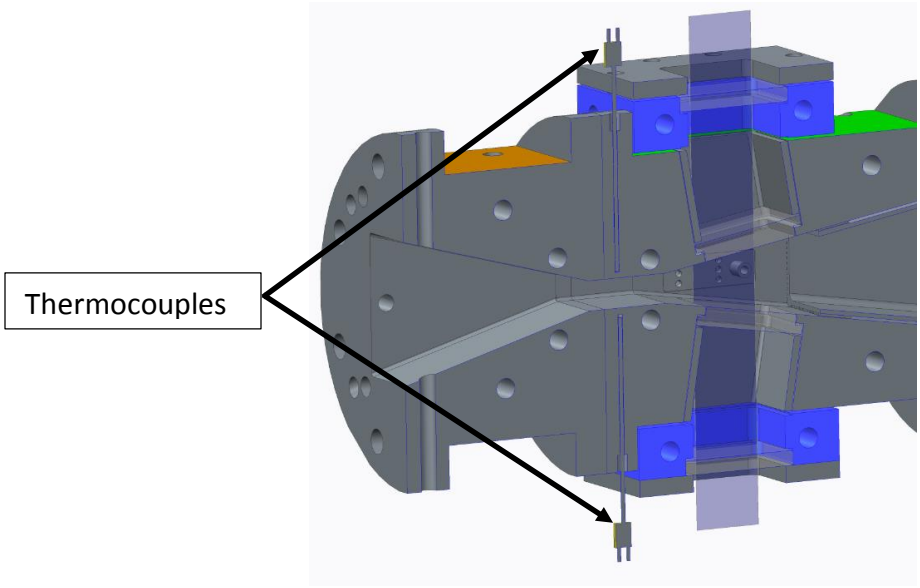

Figure 3.7: Thermocouple locations in the accelerating DCS.

3.2.3.5 Expansion Section and Quenching

The expansion section has been designed to expand high-temperature gases back to the original cross-sectional area. The expansion angle of 13.9^{o} is gradual compared to contraction angle of 17.3^{o} in the secondary combustion zone in order to avoid flow separation and shock formation. Figure 3.8 shows the expansion section having an exit

area equal to the inlet area of secondary combustion zone but longer in length due to gradual contraction angle.

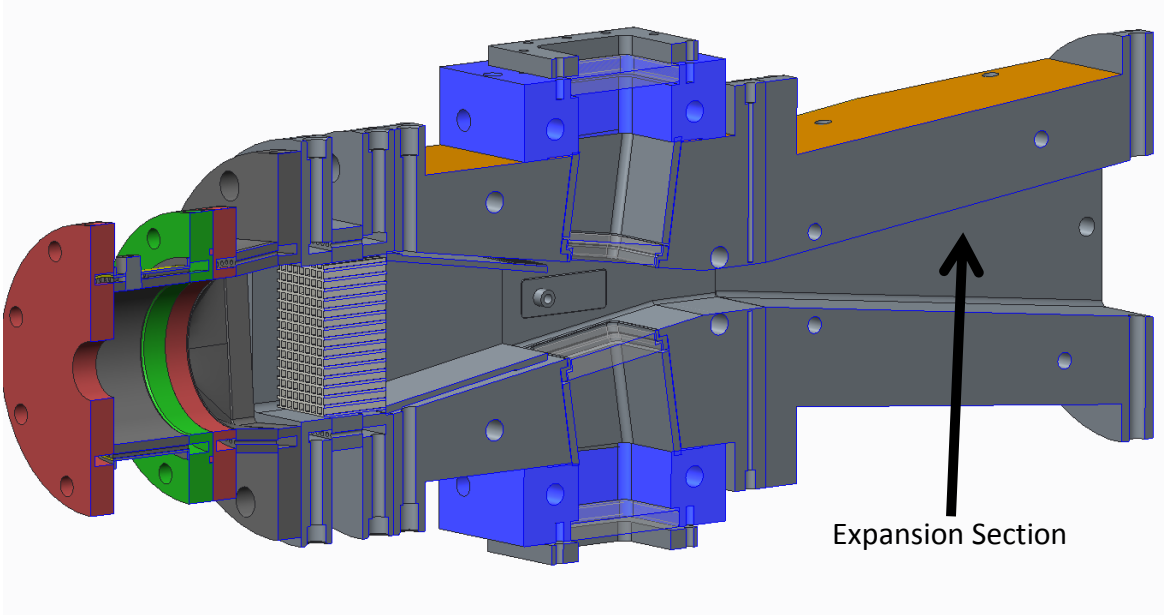

Figure 3.8: Expansion Section in the accelerating DCS.

3.2.4 Final Design

The CAD model and major dimensions of the final assembly of accelerated distribution combustion system are depicted below in Fig 3.9 and Fig 3.10.

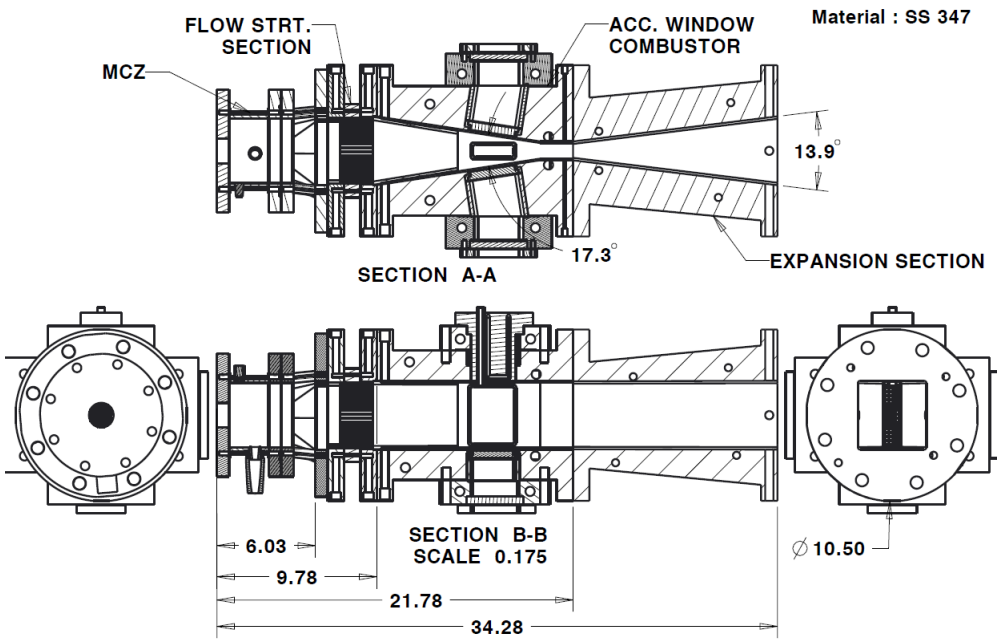

Figure 3.9: CAD representation of final design.

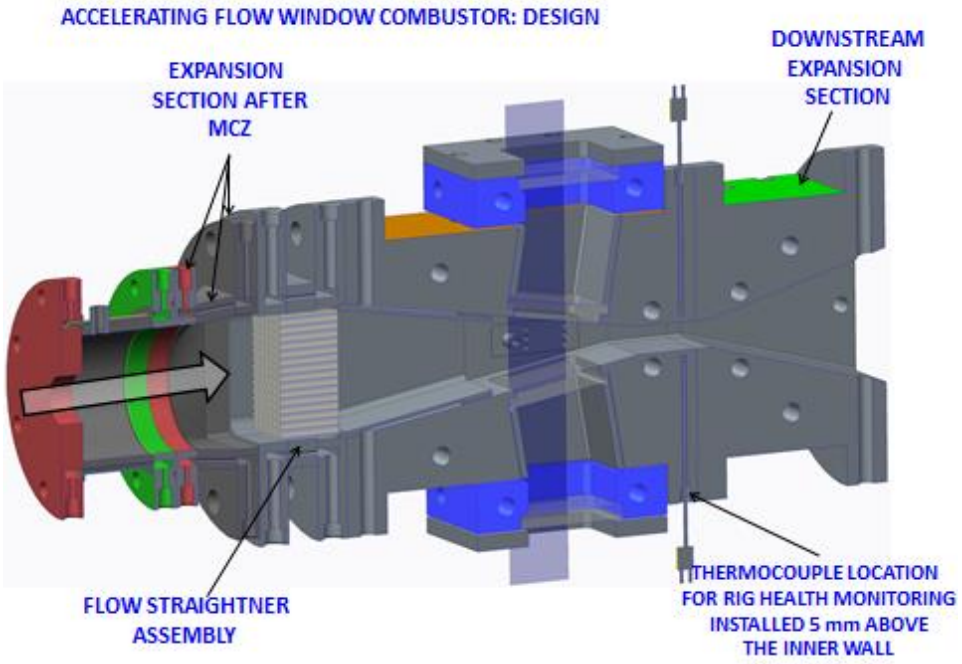

Figure 3.10: Cross-section view of the final design.

3.3 Heat Transfer Analysis

Design iterations were performed in order to meet the following design constraints:

(a) Maximum Stainless Steel 347 wall temperature of 1150 K

(b) Maximum cooling water temperature of 373 K

(c) Maximum thermal barrier coating (TBC) service temperature of 1550 K

(d) Maximum water flow rate of 10 gpm

Figure 3.11 depicts a schematic diagram of the heat transfer model used in the analysis. Heat flux from the combustion gases to the TBC liner is due to radiation (R1) and convection (C1). The heat flux across the TBC liner and SS347 metal is due to conduction (K), whereas the heat flux from SS347 metal to the water is due to convection (C2).

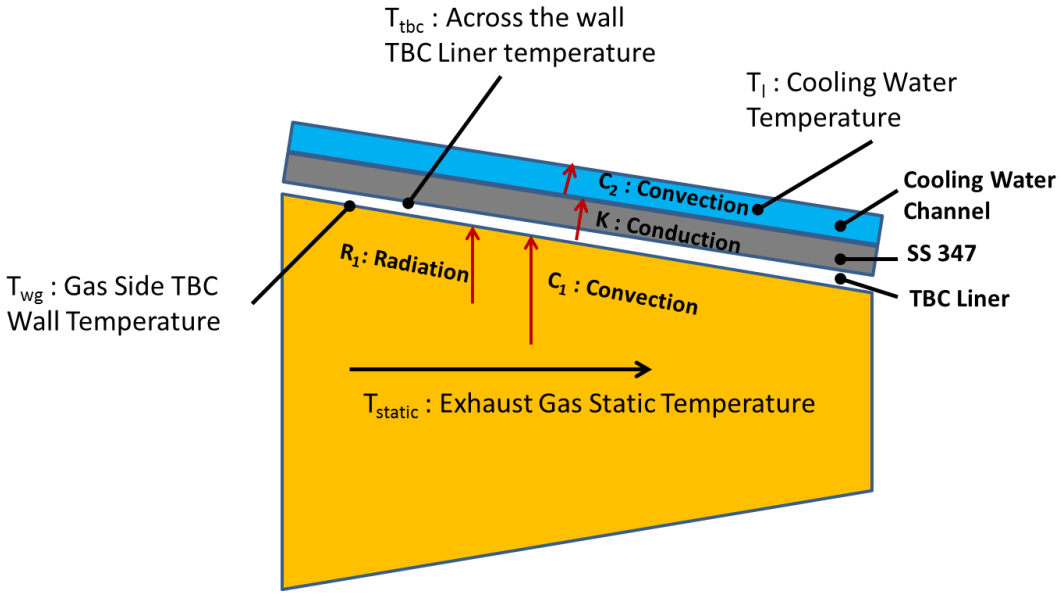

Figure 3.11: Schematic diagram of the heat transfer model.

At steady state, using the first law of thermodynamics, heat transfer into the combustor wall with internal surface area A_{wg} must be equal to heat transfer out of gases. An important assumption of negligible "stray" heat transfer is considered for estimating the safest rig operation parameters.

$$(C_1 + R_1)A_{wg} = K_{wg-tbc}A_{wg} = K_{tbc-wl}A_{tbc-wl} = C_2A_{wl} \quad (3.1)$$

In Eqn. (3.1), R_1 is the radiative heat flux from the combustion gas, C_1 is the convective heat flux from the combustion gas, K is the conductive heat flux through the combustor wall, and C_2 is the convection heat flux to the cooling water. The subscripts of (wg – tbc) and (tbc – wl) refer to the conduction across the TBC and stainless steel wall respectively.

The heat flux from the hot combustion gases to the combustor liner was calculated using the following relationships [9]

$$C_1 = 0.017\frac{k_g}{D_L^{0.2}}\left(\frac{\dot{m}}{A_L\mu_g}\right)^{0.8}(T_r - T_{\omega g}) \quad (3.2)$$

$$R_1 = 0.5\sigma(1 + \in_{\omega})\epsilon_g T_g^{1.5}(T_g^{2.5} - T_{\omega g}^{2.5}) \quad (3.3)$$

$$q'' = R_1 + C_1 \quad (3.4)$$

$$T_r = T_{static}\left[1 + \left(\frac{\gamma-1}{2}\right)\mathrm{Pr}^{\frac{1}{3}}M^2\right] \quad (3.5)$$

In Eqns. (3.2), (3.3), (3.4), and (3.5), k_g is the thermal conductivity of the exhaust gases, $T_{\omega g}$ is the gas side wall temperature, $D_L$is the combustor liner diameter, $\dot{m}$ is the mass flow rate of combustion gases, A_L is the combustor cross-sectional area, μ_g is the dynamic viscosity of exhaust gases, σ is the Stefan-Boltzmann constant, $\in_{\omega}$ is the wall

emissivity, ϵ_g is the emissivity of the combustion gases, T_r is the recovery temperature, γ is isentropic exponent, Pr is the Prandtl number, and M is the Mach number.

The following relationships were used for the conductive heat transfer across the TBC liner and SS 347:

$$q'' = \frac{k_{tbc}}{t_{tbc}}\left(T_{\omega g} - T_{tbc}\right) \tag{3.6}$$

$$q'' = \frac{k_{\omega}}{t_{\omega}}\left(T_{tbc} - T_{\omega l}\right) \tag{3.7}$$

In Equations (3.6) and (3.7), T_{tbc} is the temperature at the backside of TBC in contact with the stainless steel and $T_{\omega l}$ is the wall temperature at the backside of the stainless steel which is in contact with liquid cooling water.

Finally, the heat flux across the cooling water was calculated according to the following forced convection relationship [9]:

$$h_l = 0.027\frac{k_l}{D_h}Re_l^{4/5}Pr_l^{1/3}\left(\frac{\mu}{\mu_{\omega l}}\right)^{0.14} \tag{3.8}$$

$$C_2 = h_l(T_{\omega l} - T_l) \tag{3.9}$$

In Eqns. (3.8) and (3.9), D_h represents the hydraulic diameter of the water cooling passage, μ is the dynamic viscosity, and Re is the Reynolds number.

3.3.1 Main Combustion Zone

Calculations were performed in order to determine cooling water flow rates. In the main combustion zone, the trends in Figs. 3.12 and 3.13 show the temperatures experienced by TBC at ignition and steady state respectively. High pressure water at 5.5 bar with a volumetric flow rate of 9.5 gpm is passed through the 72 ports shown in Fig. 3.14. Results show that the water temperature will stay below 320 K, thus allowing

suitable safety margin from the boiling point. The equilibrium and frozen lines represent infinitely fast chemical reactions and infinitely slow (frozen) chemical reactions respectively.

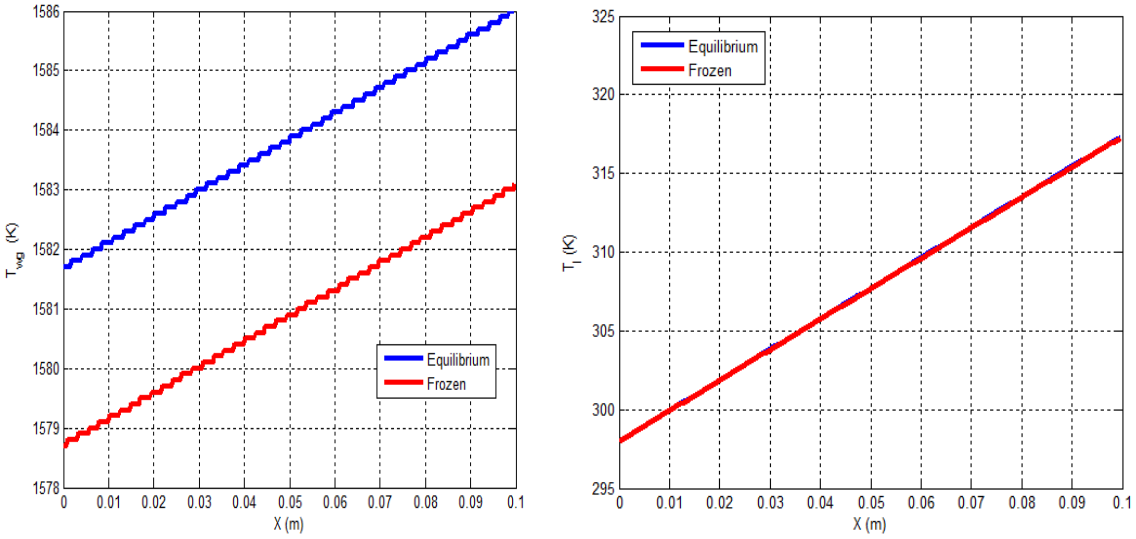

Figure 3.12: Ignition temperatures for the main combustion zone.

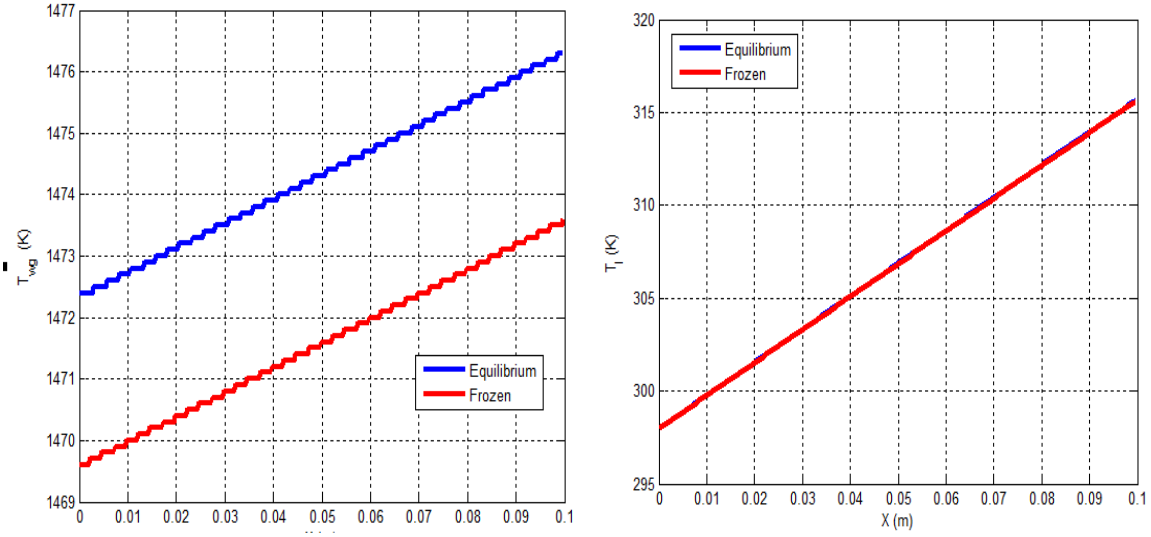

Figure 3.13: Steady state temperatures for the main combustion zone.

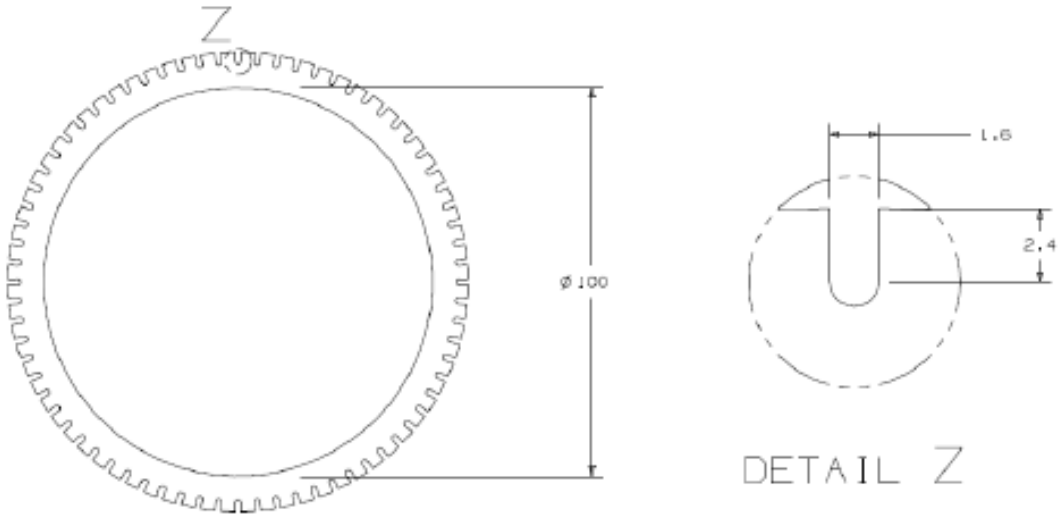

Figure 3.14: Water cooling ports for the main combustion zone.

3.3.2 Accelerating Passage (Secondary Combustion Zone)

In the secondary combustion zone, Figs. 3.15 and 3.16 show the temperatures scales experienced by thermal barrier coating at ignition and steady state respectively. Low-pressure water at 8.5 gpm will be passed through 12 channels as shown in Fig. 3.17. The trends depict that the water temperature will remain below 335 K, thus allowing a suitable safety margin compared to the boiling point.

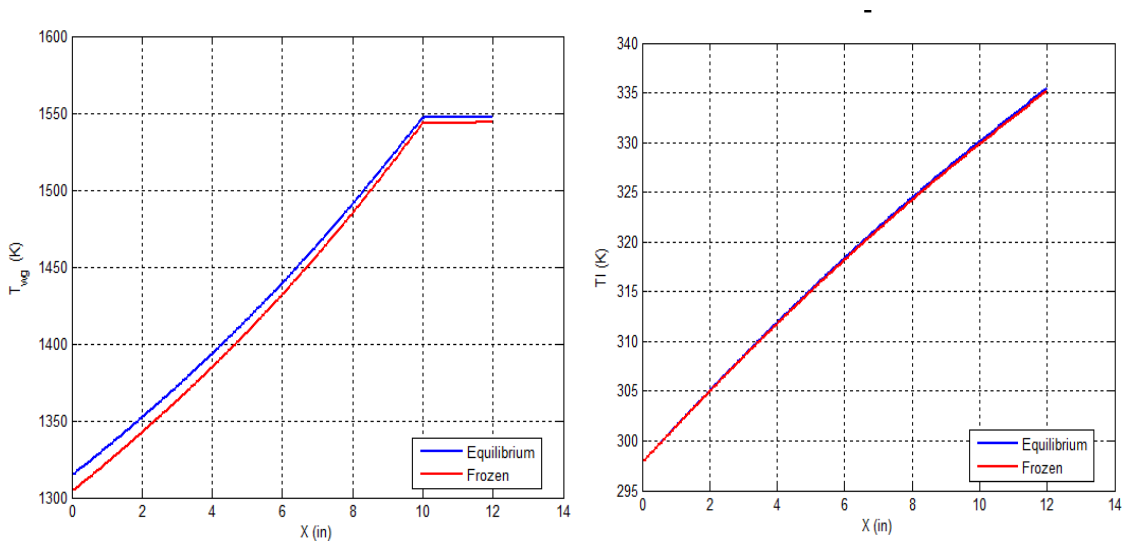

Figure 3.15: Ignition temperatures for the secondary combustion zone.

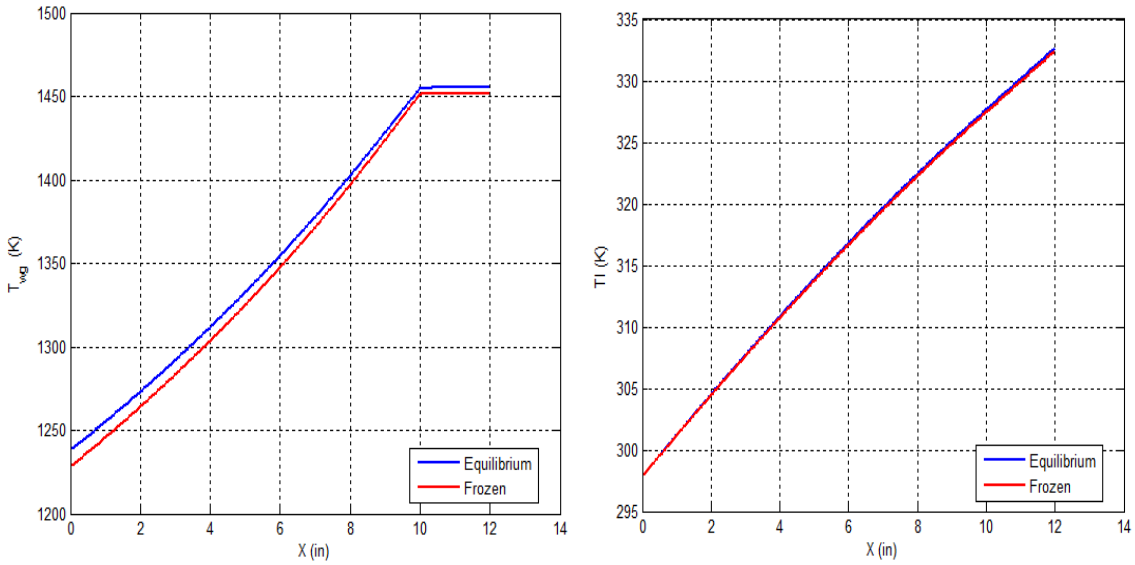

Figure 3.16: Steady state temperatures for the secondary combustion zone.

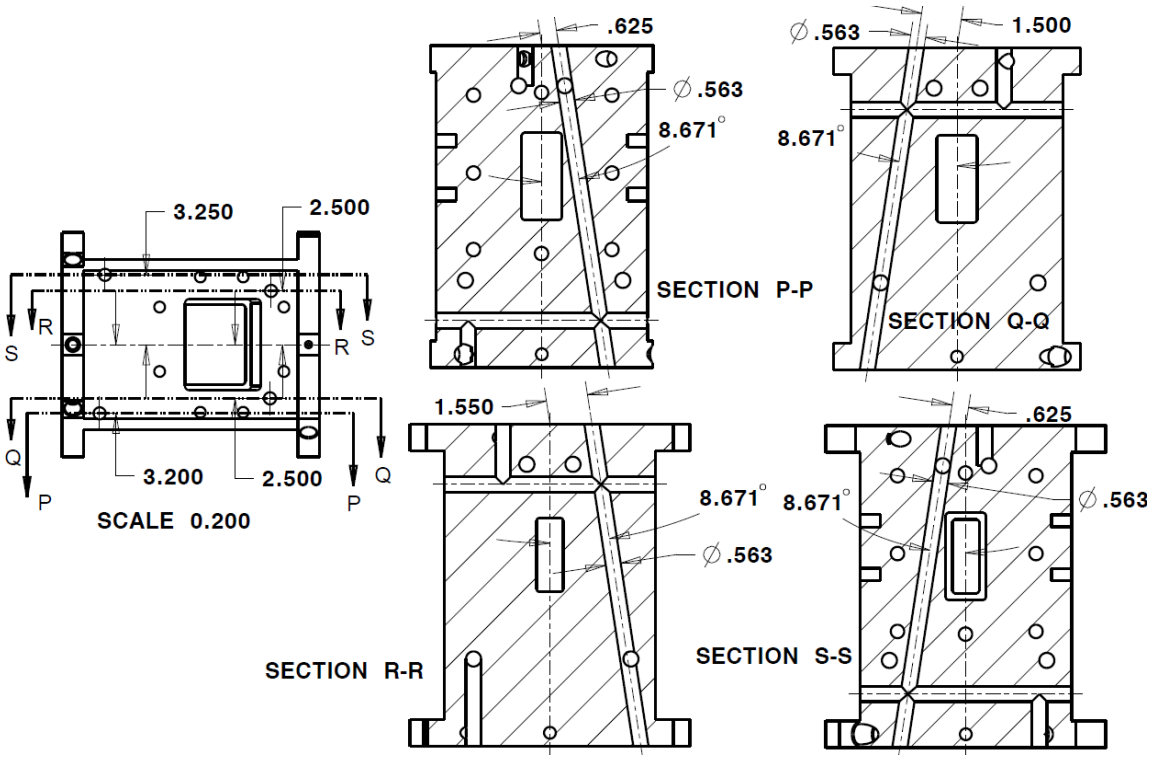

Figure 3.17: Cooling channels in the SCZ of accelerating DCS.

CHAPTER 4. CONCLUSIONS AND FUTURE WORK

4.1 Conclusion

A conceptual and detailed design of an accelerating distributed combustion system has been presented. Jets injected into the main flow which is at a Mach number of 0.3 can be visualized. A converging length of 10” followed by a straight passage of 2” was chosen for this design which will be fabricated out of Stainless Steel 347. Salient design features of windows, thermocouples, expansion section, and film cooling louvre have been discussed.

Along with the design a detailed one-dimensional heat transfer analysis was performed in order to determine cooling water flow rate of 9.5 gpm in the main combustion zone and 8.5 gpm in the secondary combustion zone. Conduction, convection, and radiation at steady state were used for determining heat transfer relationships between different materials.

Various laser diagnostic techniques such as PLIF, PIV, CARS along with emissions sampling will be performed in the future for studying combustion.

4.2 Future Work

Non-intrusive laser diagnostic techniques will be used for gathering temperature, species, and mixture fraction data in the secondary combustion zone. Emissions sampling

will be performed downstream of secondary combustion zone for measuring NOx and CO levels along with other gases.

4.2.1 High Repetition Rate Planar Laser-Induced Flourescence (PLIF)

PLIF will be used to map the reaction zone of the secondary jet. A schematic representation of the experimental arrangement is shown in Fig. 4.1.

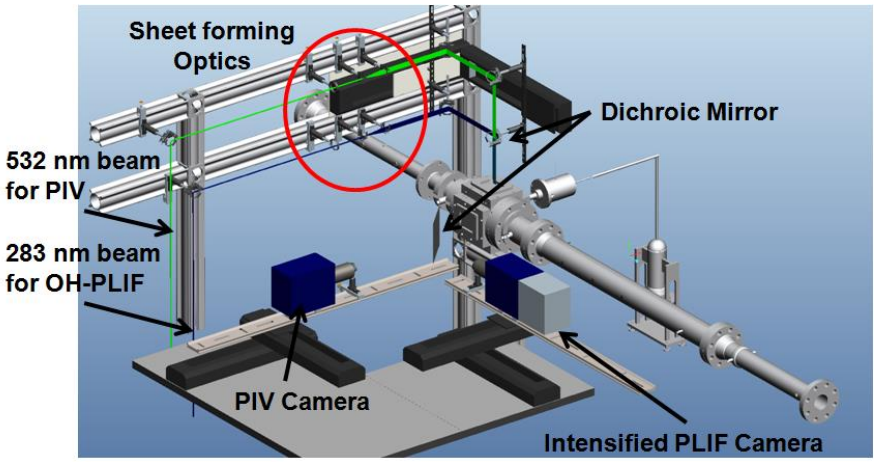

Figure 4.1: High repetition rate PLIF arrangement.

4.2.2 High Repetition Rate Particle Image Velocimetry (PIV)

High repetition rate PIV will be performed to obtain length scale and time scale data of turbulent reacting flows. A CAD representation of the experimental system is shown in Fig. 4.2.

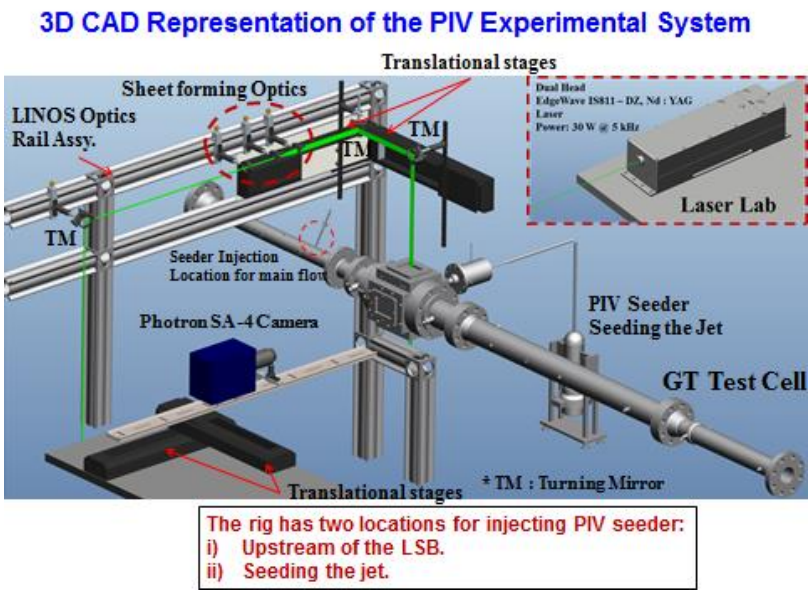

Figure 4.2: High repetition rate PIV arrangement.

4.2.3 Emissions Sampling

Emissions sampling will be performed using a Flame Ionization Detector (FID) and a Fourier Transform Infrared Spectrometer (FTIR). Unburned hydrocarbon emissions will be measured using the FID, whereas, carbon dioxide, carbon monoxide, water-vapor, nitric oxide, and nitrogen dioxide will be measured using FTIR. A sensor to FTIR will also allow measurement of oxygen.

4.3 Future Modifications

In the current design, a Mach number of 0.3 can be visualized in the accelerating combustion system. The nozzle position can be changed to visualize secondary combustion at different Mach numbers. This can be done by having multiple injector flanges having injector located at known distances from upstream in order to inject the

secondary fuel at different Mach numbers. In Fig. 4.3, various positions of injector nozzle are shown.

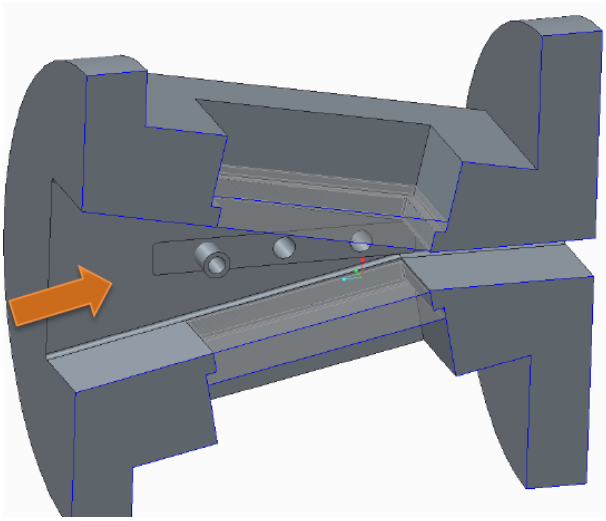

Figure 4.3: Multiple injector locations.

LIST OF REFERENCES

LIST OF REFERENCES

[1] J. Melillo, T. Richmond, and G. Yohe. Highlights of Climate Change Impacts in the United States: The Third National Climate Assessment. U.S. Global Change Research Program, 2014

[2] R. Jones. Advanced technology for reducing aircraft engine pollution. In American Society of Mechanical Engineers, Winter Annual Meeting, Detroit, Michigan, NASA-sponsored research, volume 96, 1973.

[3] GE Energy. 7FA Heavy Duty Gas Turbine, 2011.

[4] Siemens Energy. Siemens Gas Turbine SGT6-5000F, 2011.

[5] W. Lamont. Experimental study of a staged combustion system for stationary gas turbine applications. PhD Thesis, Purdue University, 2012.

[6] M. Roa. Investigation of reacting jet injected into vitiated crossflow using CARS, high repetition rate OH-PLIF, and high repetition rate PIV. PhD Thesis, Purdue University, 2014

[7] H. Mongia. Engineering aspects of complex gas turbine combustion mixers part III: 30 OPR. In 9th Annual International Energy Conversion Engineering Conference, San Diego, California, 2011.

[8] W. Lamont, M. Roa, S. Meyer, and R. Lucht. Emission Measurements and CH Chemiluminescence of a Staged Combustion Rig for Stationary Gas Turbine Applications. Journal of Engineering for Gas Turbines and Power, 134(8):081502, 2012.

[9] A. Lefebvre. Gas Turbine Combustion. Taylor & Francis, 2nd edition, 1999.

APPENDICES

Appendix A

```
% MATLAB code for heat transfer analysis when the rocket chamber and
nozzle are cooled using turbine exhaust gases.
% Originally written by Warren Lamont, modified by Yashovardhan Wagh
and
% Pratikash Panda for new design
clear all;
close all;
tic

disp(sprintf('\n phi = 0.5, 5 bar, nominal, head end case, See
\CEA\siemens.out for CEA %s\n'));
disp(sprintf('\n Starting Calculation... %s\n'));


% To      =   1792;         %was 1964                    %stagnation
temperature K (adiabatic ~ 2000 K)
P       =   550000;                                     %static pressure
(Pa)
% rho     =   1.0478;                                     %kg/m^3
% % V       =   mg/(rho*pi*R^2);                          %gas
velocity m/s
% ag      =   816.6;                                      %speed of
sound m/s
 MUG     =   0.000064895;                                %kg/sm
gamma   =   1.2667;                                     %in the
combustion chamber
R_g     =   287;
Rgas    =   287;
% M       =   V/ag;                                       %mach number
of exhaust gas
% Reg     =   rho*M*ag*2*R/MUG;                           %gaseous
reynolds number
% Po      =   (1+(gamma-1)/2*M^2)^(gamma/(gamma-1))*P;    %stagnation
pressure;



%Intialization
nmax = 250
To = 1800; %SCZ Inlet temperature in K.
Pcomb = 550000; %Combustion operating Pressure Pa.
mdot_main = 1.25; %MCZ+SCZ+N2 Film Cooling mass flow rate in kg/s.

mdotl = 1.2; % Mass flow rate of cooling water kg/s 9.5 gpm conversion
kg/s = 60/3.8 gpm
M_exit = 0.8; %Exit Mach # 0.8.
x = zeros(nmax,1);
y = zeros(nmax,1);
A = zeros(nmax,1); %Cross-Section of the combustor
```

```
Pstatic = zeros(nmax,1);
Tstatic = zeros(nmax,1);
rho = zeros(nmax,1);
M = zeros(nmax,1); %Mach Number
C = zeros(nmax,1); %Speed of Sound
V = zeros(nmax,1); %Velocity of Exhaust Gas
Prcomb = zeros(nmax,1); %Combustor Perimeter
Dhy = zeros(nmax,1); %Comb hydrualic diameter
H_inlet = 0.1067; %Inlet Height of the combustor H = 4.2 in.

H_exit = 0.022; % ** Exit Height of the combustor H = 0.88 in
                %check  and change as per the length and convergence
angle

D_comb = 0.1067; %SCZ Depth D = 4.2 in, injector to wall distance kept
constant.
% L_conv =  0.2032; %Length of the convergin section L= 8 in.
% L_strgt = 0.1016; %Length of the convergin section L= 4 in.
L_conv =  0.254; %Length of the convergin section L= 10 in.
L_strgt = 0.0508; %Length of the convergin section L= 2 in.
L_tot = 0.3048; %Total Length of Combustor, L = 12 in.
% theta_conv = 11.7*pi()/180; %Convergence Half Angle 11.7 degree.
theta_conv = 9.5*pi()/180; %Changing the half angle to 9.8 degree.
% nmax = 1000;
delta = L_tot/nmax;

% Contour of the Window Combustor.
for i=1:nmax
    x(i)=i*delta;
    if x(i)<=L_conv
        y(i)= H_inlet - 2*tan(theta_conv)*(x(i));
        A(i)=y(i)*D_comb;
        Prcomb(i)=2*(y(i)+D_comb);
        Dhy(i) = 4*A(i)/Prcomb(i);
    else
        y(i)=H_exit;
        A(i)=y(i)*D_comb;
        Prcomb(i)=2*(y(i)+D_comb);
        Dhy(i) = 4*A(i)/Prcomb(i);
    end
end

%SCZ Inlet Condition Calculation
A_inlet = H_inlet*D_comb;
rho_inlet = Pcomb/Rgas/To;
V_inlet = mdot_main/rho_inlet/A_inlet;
C_inlet = sqrt(gamma*Rgas*To);
M_inlet = V_inlet/C_inlet;

Po=Pcomb*(1+((gamma-1)/2)*M_inlet^2)^((gamma)/(gamma-1));
%Area Calculation at all the converging stations.
% del_Mach = ((M_exit-M_inlet)/(nmax*(L_tot-L_strgt)/L_tot));
Lconv_exit = (L_tot-L_strgt)/L_tot;
M_guess = 0.1;
```

```
for i=1:nmax

    if i<nmax*Lconv_exit
        M(i)= M_guess;
        for j=1:100

            Pstatic(i)=Po/(1+((gamma-1)/2)*(M(i))^2)^((gamma)/(gamma-
1));
            Tstatic(i)=To/(1+((gamma-1)/2)*(M(i))^2);
            rho(i)=Pstatic(i)/(Rgas*Tstatic(i));
            C(i)=sqrt(gamma*Rgas*Tstatic(i));
            V(i)=M(i)*C(i);
            A(i)=mdot_main/rho(i)/V(i);
            y2=A(i)/D_comb;
            err=y2-y(i);
            if err < 0.01
                M(i)=M(i);
                break;
            else
                M(i)=M(i)+0.01;
            end
        end

    else
        M(i)=0.8;
        Pstatic(i)=Po/(1+((gamma-1)/2)*(M(i))^2)^((gamma)/(gamma-1));
        Tstatic(i)=To/(1+((gamma-1)/2)*(M(i))^2);
        rho(i)=Pstatic(i)/(Rgas*Tstatic(i));
        C(i)=sqrt(gamma*Rgas*Tstatic(i));
        V(i)=M(i)*C(i);
%         A(i)=mdot_main/rho(i)/V(i);
%         y(i)=A(i)/2/D_comb;
    end

end

% figure()
% subplot(2,2,1)
%     plot(x/0.0254,y/2/0.0254);
%     hold on;
%     plot(x/0.0254,-y/2/0.0254);
% xlabel('X (in)');
% ylabel('Hcomb (in)');
% grid;
% subplot(2,2,2)
%     plot(x/0.0254,M);
% xlabel('X (in)');
% ylabel('Ma #');
% grid;
% subplot(2,2,3)
%     plot(x/0.0254,rho);
% xlabel('X (in)');
% ylabel('Gas Density (kg/m^3)');
% grid;
```

```
% subplot(2,2,4)
%     plot(x/0.0254,V);
% xlabel('X (in)');
% ylabel('Velocity (m/s)');
% grid;


%Plotting Variables
% Create figure
figure1 = figure('Color',[1 1 1]);

% Create subplot
subplot1 =
subplot(2,2,1,'Parent',figure1,'FontWeight','bold','FontSize',20,...
    'FontName','Times New Roman');
box(subplot1,'on');
grid(subplot1,'on');
hold(subplot1,'all');

% Create multiple lines using matrix input to plot
plot(x/0.0254,y/2/0.0254,'Parent',subplot1,'LineWidth',4);
hold on;
plot(x/0.0254,-y/2/0.0254,'Parent',subplot1,'LineWidth',4);
% Create xlabel
xlabel('X (in)','FontWeight','bold','FontSize',20,...
    'FontName','Times New Roman');

% Create ylabel
ylabel('Hcomb (in)','FontWeight','bold','FontSize',20,...
    'FontName','Times New Roman');

% Create subplot
subplot2 =
subplot(2,2,2,'Parent',figure1,'FontWeight','bold','FontSize',20,...
    'FontName','Times');
box(subplot2,'on');
grid(subplot2,'on');
hold(subplot2,'all');

% Create plot
plot(x/0.0254,M,'Parent',subplot2,'LineWidth',4);

% Create xlabel
xlabel('X (in)','FontWeight','bold','FontSize',20,...
    'FontName','Times New Roman');

% Create ylabel
ylabel('Ma #','FontWeight','bold','FontSize',20,...
    'FontName','Times New Roman');

% Create subplot
subplot3 =
subplot(2,2,3,'Parent',figure1,'FontSize',20,'FontName','Times');
```

```
box(subplot3,'on');
grid(subplot3,'on');
hold(subplot3,'all');

% Create plot
plot(x/0.0254,rho,'Parent',subplot3,'LineWidth',4);

% Create xlabel
xlabel('X (in)','FontWeight','bold','FontSize',20,...
    'FontName','Times New Roman');

% Create ylabel
ylabel('Gas Density (kg/m^3)','FontWeight','bold','FontSize',20,...
    'FontName','Times New Roman');

% Create subplot
subplot4 =
subplot(2,2,4,'Parent',figure1,'FontSize',20,'FontName','Times');
box(subplot4,'on');
grid(subplot4,'on');
hold(subplot4,'all');

% Create plot
plot(x/0.0254,V,'Parent',subplot4,'LineWidth',4);

% Create xlabel
xlabel('X (in)','FontWeight','bold','FontSize',20,...
    'FontName','Times New Roman');

% Create ylabel
ylabel('Velocity (m/s)','FontWeight','bold','FontSize',20,...
    'FontName','Times New Roman');




%exhaust gas fluid properites:
%  To      =   1800;           %   Temperature coming into window
combustor assuming head end of 0.55 equi ratio  1964;  %stagnation
temperature K (adiabatic ~ 2000 K)
% P       =   550000;                                    %static
pressure (Pa)
% rho     =   1.0268;                                     %kg/m^3
% V       =   mg/(rho*pi*R^2);                            %gas velocity
m/s
% ag      =   824;                                       %speed of sound
m/s
%  MUG     =   0.000065769;                                %kg/sm
%  gamma   =   1.2530;                                     %in the
combustion chamber
% M       =   V/ag;                                       %mach number
of exhaust gas
```

```
% Reg     =   rho*M*ag*2*R/MUG;                              %gaseous
reynolds number
% Po      =   (1+(gamma-1)/2*M^2)^(gamma/(gamma-1))*P;    %stagnation
pressure;

Eg      =   0.26;           %gas emissivity from calculations in black
book for non luminous exhaust gas
Ew      =   0.984;          %Emissivity for 8YSZ TBC   %wall emissivity
from Lefebvre page 278 for SS 0.8
SB      =   5.67e-8;        %Stefan-Boltzmann Constant W/m^2K^2
Ess     =   0.8;            %** Look up for SS 347.  emissivity of
Stainless Steel 316/SS 347.

%wall conductivity  SS316 @ 800 K [incropera & dewitt]
%** Look Up wall conductivity  SS347 @ 800 K [incropera & dewitt]
kw      =   21.3; %W/mK
tw      =   6e-3; %[m] wall thickness ** Can change upto 10 mm.
Tl(1)   =   298; %[K] manifold temperature
% Ta(1)      = 240; %[K] N2 comes in cold because of expansion.

%properties of TBC (assumed)
ttbc    =   0.0005;  %m   (500 um) 100um bond coat and 400 um TBC layer
ktbc    =   1.2; %W/mK    from Anand Kulkarni

%Nitrogen properties (annulus)
ka      =   0.0259;         %W/mK conductivity for N2 at 300 K
Dan     =   2*0.000965;%508;     %for an annular chamber page 282 from
Lefebvre
% man     =   0.025675;       %kg/s N2 flow. 10% of bulk flow
man     =   0.75/2.2;       %kg/s N2 flow. 10% of bulk flow
Aan     =   3.09*10^(-4);  %area required to match velocities
mua     =   178.2*10^-7;    %Ns/m^2 viscosity at 300 K
cpa     =   1.041*1000;     %J/kgK

% %coolant is water and assumed constant properties (no phase change)
cpl     =   4180; %J/kgK
kl      =   0.58;  %W/mK
mul     =   0.000548; %kg/ms
rhol    =   988; %kg/m^3
Cc      = 12; % Number of cooling passages.
% Perl    =   ((0.0625+2*0.09375)+pi*0.0625/2)*0.0254;       %perimeter
of one cooling channel m
% Al      =   ((0.0625*0.09375)+pi/8*0.0652^2)*0.0254^2;   %area of one
cooling channel m^2
dl      =   0.6*0.0254; %Size of cooling passage 0.5"
Perl    =   2*pi*dl;       %perimeter of one cooling channel m
Al      =   pi/4*dl^2;   %area of one cooling channel m^2
Dh      =   4*Al/Perl;
Rel     =   4*(mdotl/Cc)/Perl/mul;
Prl     =   mul*cpl/kl;
%%

%Expansion conditions designator (1= equilibrium, 2= frozen);
```

```
% for eqfz=1:2;
%
%         if eqfz == 1    %eq'm
%             Kg=1.2633; %W/mk;
%             PRg=0.7349;
%         elseif  eqfz==2
%             Kg=1.2102; %W/mk
%             PRg=0.7399;
%         else
%         break
%         end
%     for i=1:nmax
%
%
%


%     end
% end


%%

last = nmax;
for eqfz=1:2;

        if eqfz == 1    %eq'm
            Kg=1.2633; %W/mk;
            PRg=0.7349;
        elseif  eqfz==2
            Kg=1.2102; %W/mk
            PRg=0.7399;
        else
            break
        end
for ind=1:nmax
    qdot1(ind)=1e30;
    qdot2(ind)=1;
    i(ind)=1;
    increment=0.1;
    limit=20000;
    err = 5000;

    %Recovery Temperature for HTC calculation
%       Tr(ind)      =   To/(1+(gamma-1)/2*PRg^(1/3)*M(ind)^2);
       Tr(ind)      =   Tstatic(ind)*(1+(gamma-
1)/2*PRg^(1/3)*M(ind)^2);


    % %internal convection from Lefebvre:
    hg(ind)      =
0.017*Kg/((Dhy(ind))^0.2)*(mdot_main/(A(ind)*MUG))^0.8;
```

```
    Twg(ind)=700;       %guess
    while abs(qdot1(ind)-qdot2(ind))>err && i(ind)<limit
        qdot1(ind)=hg(ind)*(Tr(ind)-
Twg(ind))+0.5*SB*(1+Ew)*Eg*To^1.5*(To^2.5-Twg(ind)^2.5);
        Ti(ind)=Twg(ind)-qdot1(ind)*ttbc/ktbc;
        Twl(ind)=Ti(ind)-qdot1(ind)*tw/kw;
        [muwl]= propliq(Twl(ind));
        %Sieder and Tate for large proper variation in turbulent tubes

hl(ind)=kl/(4*Al/Perl)*0.027*(Rel)^0.8*Prl^(1/3)*(mul/muwl)^0.14;
        if ind ==1
            qdot2(ind)=hl(ind)*(Twl(ind)-Tl(ind));
        else
            qdot2(ind)=hl(ind)*(Twl(ind)-Tl(ind-1));
        end
        Twg(ind)=Twg(ind)+increment;
        i(ind)=i(ind)+1;
        error(ind)=abs(qdot1(ind)-qdot2(ind));
      end
    X=L_tot/nmax;
    %calculate Tli from Tl-1
    if ind==1
        %do nothing assumed the first point uses the manifold
temperature
    elseif ind == last
        Tl(ind)=Tl(ind-
1)+1/(mdotl/Cc*cpl)*(X/2)*qdot2(ind)*((Prcomb(ind))/Cc);  %72 cooling
channels
    else
        Tl(ind)=Tl(ind-
1)+1/(mdotl/Cc*cpl)*(X)*qdot2(ind)*((Prcomb(ind))/Cc);
    end

end
%%

% %determine presure drop
% Pl(1)=413685.44;    %pressure [pa] in manifold 60 psi
% q=(mdotl/Cc)^2/(2*rhol*(Al)^2);
% f=0.0014+0.125/Rel^0.32;
% for ind=2:(last)
%     Pl(ind)=Pl(ind-1)-(4*f*X/(4*Al/Perl)*(q));
% end


%P=P/6894.7573;  %convert pressure to PSI
%q=q/6894.7573;  %convert dynamic pressure to psi
%exporting part ii
% C(1,:)={'Segment','X [m]', 'r [m]','S [m]', 'M', 'P [psi]', 'T [K]'};
% cellwrite('output.txt',C);
% for y=1:length(X)
%     B(y,:)={y,X(y),R(y),S(y),M(y),P(y),T(y)};
% end
% cellwrite('output.txt',B);
```

```
%
%Pl=Pl/6894.7573;    %convert liquid pressure drop to PSI
% %exporting2 part iii
% D(1,:)={'Segment','X [m]', 'r [m]','$P_l$ [Pa]',
'$\dot{q}$ [W/$m^2$]','$h_g$ [W/$m^2$K]','$h_l$ [W/$m^2$K]',
'$T_l$ [K]', '$T_{wg}$ [K]'};
% cellwrite('output2.txt',D);
% for y=1:length(X)
%     E(y,:)={y,X(y),R(y),Pl(y),qdot1(y),hg(y),hl(y),Tl(y),Twg(y)};
% end
% cellwrite('output2.txt',E);
%
QDOT(:,eqfz)=qdot1;
HG1(:,eqfz)=hg;
%HL1(:,eqfz)=hl;
TL(:,eqfz)=Tl;
TWG(:,eqfz)=Twg;
TWL(:,eqfz)=Twl;
I(:,eqfz)= i;
TI(:,eqfz) = Ti;
ERROR(:,eqfz)=error;
%PL1(:,eqfz)=Pl;
%
end
%
%
% (PL1(1,1)-PL1(last,1))/6894.7573
% (PL1(1,2)-PL1(last,2))/6894.7573
%
%%
tplot(1,:)=['equilibrium','frozen'];
 color(1,:)='b- ';
 color(2,:)='r- ';
% color(3,:)='r-.';
% color(4,:)='c--';

% figure(1)
% for v=1:2
%     plot(S,PL1(:,v),color(v,:),'LineWidth',2);
%     hold on;
% end
% legend('Equilibrium','Frozen','Location','Best');
% xlabel('X (m)');
% ylabel('Pl (Pa)');
% grid;

%
figure(2)
for v=1:2
    plot(x/0.0254,QDOT(:,v),color(v,:),'LineWidth',2);
    hold on;
end
legend('Equilibrium','Frozen','Location','Best');
xlabel('X (in)');
ylabel('qdot (W/m^2)');
```

```
grid;
%
% figure(3)
% for v=1:2
%     plot(X,HG1(:,v),color(v,:),'LineWidth',2);
%     hold on;
% end
% legend('Equilibrium','Frozen','Location','Best');
% xlabel('X (m)');
% ylabel('h_g (W/m^2K)');
% grid;
%
% figure(4)
% for v=1:2
%     plot(X,HL1(:,v),color(v,:),'LineWidth',2);
%     hold on;
% end
% legend('Equilibrium','Frozen','Location','Best');
% xlabel('X (m)');
% ylabel('h_l (W/m^2K)');
% grid;
%
figure(5)
for v=1:2
    plot(x/0.0254,TL(:,v),color(v,:),'LineWidth',2);
    hold on;
end
legend('Equilibrium','Frozen','Location','Best');
xlabel('X (in)');
ylabel('Tl (K)');
grid;
%
figure(6)
for v=1:2
    plot(x/0.0254,TWG(:,v),color(v,:),'LineWidth',2);
    hold on;
end
legend('Equilibrium','Frozen','Location','Best');
xlabel('X (in)');
ylabel('T_{wg} (K)');
grid;

figure(7)
for v=1:2
    plot(x/0.0254,TWL(:,v),color(v,:),'LineWidth',2);
    hold on;
end
legend('Equilibrium','Frozen','Location','Best');
xlabel('X (in)');
ylabel('T_{wl} (K)');
grid;

figure(8)
for v=1:2
    plot(x/0.0254,TI(:,v),color(v,:),'LineWidth',2);
```

```
    hold on;
end
legend('Equilibrium','Frozen','Location','Best');
xlabel('X (in)');
ylabel('T_{TBC} (K)');
grid;
figure1 = figure('Color',[1 1 1]);

for i=1:2
% Create axes
axes1 = axes('Parent',figure1,'FontWeight','bold','FontSize',20,...
    'FontName','Times');
box(axes1,'on');
grid(axes1,'on');
hold(axes1,'all');

% Create multiple lines using matrix input to plot
plot1(i) =
plot(x/0.0254,TI(:,v),color(v,:),'Parent',axes1,'LineWidth',4);
set(plot1(1),'Color',[0 0 1],'DisplayName','Equilibrium');
set(plot1(2),'Color',[1 0 0],'DisplayName','Frozen');

% Create xlabel
xlabel('X (in)','FontWeight','bold','FontSize',20,'FontName','Times');

% Create ylabel
ylabel('qdot
(W/m^2)','FontWeight','bold','FontSize',20,'FontName','Times');

% Create legend
legend1 = legend(axes1,'show');
set(legend1,'Location','Best');
end
%
% figure(7)
% plot(X,RHOL)
% xlabel('X (m)');
% ylabel('\rho_l (kg/m^3)');
% grid;
%
% figure(8)
% plot(X,MUL)
% xlabel('X (m)');
% ylabel('\mu_l (kg/ms)');
% grid;

%subplot(3,2,1)
% figure (3)
%     plot(X,R, 'o');
%     xlabel('X [m]','FontSize',10)
%     ylabel('R [m]','FontSize',10)
%     grid on;
%
% subplot(3,2,2)
```

```
%     plot(X,Twg);
%     xlabel('X [m]','FontSize',10)
%     ylabel('Twg [K]','FontSize',10)
%     grid on;
%
% subplot(3,2,3)
%     plot(X,i, 'o')
%     xlabel('X [m]','FontSize',10)
%     ylabel('# of iterations for convergence','FontSize',10)
%     grid on;
%
%     subplot(3,2,4)
%     plot(X,Pl)
%     xlabel('X [m]','FontSize',10)
%     ylabel('Pl [psi]','FontSize',10)
%     grid on;
%
%     subplot(3,2,5)
%     plot(X,M)
%     xlabel('X [m]','FontSize',10)
%     ylabel('M','FontSize',10)
%     grid on;
%
%     subplot(3,2,6)
%     plot(X,Tl)
%     xlabel('X [m]','FontSize',10)
%     ylabel('Tl','FontSize',10)
%     grid on;

   % subplot(3,2,2)
% plot(t,F)
% xlabel('time [s]','FontSize',10)
% ylabel('Thrust [N]','FontSize',10)
% grid on
% subplot(3,2,3)
% plot(t,Cf)
% xlabel('time [s]','FontSize',10)
% ylabel('Cf','FontSize',10)
% grid on
% subplot


% color(1,:)='b- ';
% color(2,:)='g: ';
% color(3,:)='r-.';
% color(4,:)='c--';
% figure(1)
% for q=1:length(tplot)
%     plot(x,Tw(tind(q),:),color(q,:),'LineWidth',2);
%     hold on;
%     char(q,:)=num2str(tplot(q),'%12.3g');
%     LGD(q,:)=['t=',char(q,:),'s'];
% end
% xlabel('Wall Location (m)');
% ylabel('Temperature (K)');
```

```
% legend(LGD);
% grid;
%
% for n=1:length(Tw(:,1))
%     t2(n,1)=t(1,n);
% end
%
% figure(2)
% plot(t2,Tw(:,1));
% xlabel('Time (s)');
% ylabel('Wall Surface Temperature (K)');
% grid;
disp(sprintf('\n Finished.%s\n'));
toc
```

Appendix B

```
%Siemens HT code with pressure drop
%"It is better to live one day as a lion, than a thousand years as a
lamb."
%W. Lamont
% Originally written by Warren Lamont, modified by Yashovardhan Wagh
and
% Pratikash Panda for new design

%Head end using CEA properties from \CEA\siemens.out (NOMINAL)

%Adapting to 4" window combustor with Louvre.  This calculates the wall
%temperature of the Louvre.  N2 cooling in annulus (C2).
tic
clear all
close all
clc

disp(sprintf('\n phi = 0.6, 5 bar, nominal, louvre, See
\CEA\siemens.out for CEA %s\n'));
disp(sprintf('\n Starting Calculation... %s\n'));
%%
%read in data and convert to SI units m, m^2:
L       =   0.098;      %length in m
R       =   0.11/2;    %hydraulic radius m Dh = 4A/P
N       =   100;     %number of segments
X       =   L/N;      %length of each segment
mg      =   1.0;   %mdot of exhaust gas kg/s
% mg      =   1.25;   %mdot of exhaust gas kg/s
mdotl   =   0.37;   %mdot of water coolant ~ 4gpm (0.25 kg/s)
Cc      =   72;     %Number of cooling Channels
%%

S(1,1)=X/2;
for i =2:(N-1)
    S(i,1)=S(i-1)+X;
    i=i+1;
end
S(N)=S(N-1)+X/2;

%%
%exhaust gas fluid properites:

To      =   1900;           %   Temperature coming into window
combustor assuming head end of 0.55 equi ratio  1964;  %stagnation
temperature K (adiabatic ~ 2000 K)
P       =   550000;                                    %static pressure
(Pa)
rho     =   1.0268;                                     %kg/m^3
```

```
V       =   mg/(rho*pi*R^2);                                %gas velocity
m/s
ag      =   824;                                          %speed of sound
m/s
MUG     =   0.000065769;                                    %kg/sm
gamma   =   1.2530;                                         %in the
combustion chamber
M       =   V/ag;                                           %mach number of
exhaust gas
Reg     =   rho*M*ag*2*R/MUG;                               %gaseous
reynolds number
Po      =   (1+(gamma-1)/2*M^2)^(gamma/(gamma-1))*P;    %stagnation
pressure;

Eg      =   0.26;           %gas emissivity from calculations in black
book for non luminous exhaust gas
Ew      =   0.984;          %Emissivity for 8YSZ TBC   %wall emissivity
from Lefebvre page 278 for SS 0.8
SB      =   5.67e-8;        %Stefan-Boltzmann Constant W/m^2K^2
Ess     =   0.8;            %emissivity of Stainless Steel 316.
Tstatic=To/(1+((gamma-1)/2)*(M)^2);
%wall conductivity  SS316 @ 800 K [incropera & dewitt]
kw      =   21.3; %W/mK
tw      =   6e-3; %[m] wall thickness
%Tl(1)   =   298; %[K] manifold temperature
Ta(1)      = 240; %[K] N2 comes in cold because of expansion.

%properties of TBC (assumed)
ttbc    =   0.0005;  %m   (500 um) 100um bond coat and 400 um TBC layer
ktbc    =   1.2; %W/mK    from Anand Kulkarni

%Nitrogen properties (annulus)
ka      =   0.0259;         %W/mK conductivity for N2 at 300 K
Dan     =   2*0.000965;%508;     %for an annular chamber page 282 from
Lefebvre
% man     =   0.025675/2;       %kg/s N2 flow. 10% of bulk flow
man = 0.25; % 20% for Ma = 0.3
% Aan     =   2.122*10^(-4);  %area required to match velocities
Aan     =   2.09*10^(-4);  %area required to match velocities
mua     =   178.2*10^-7;    %Ns/m^2 viscosity at 300 K
cpa     =   1.041*1000;     %J/kgK

% %coolant is water and assumed constant properties (no phase change)
% cpl     =   4180; %J/kgK
% kl      =   0.58;  %W/mK
% mul     =   0.000548; %kg/ms
% rhol    =   988; %kg/m^3
% Perl    =   ((0.0625+2*0.09375)+pi*0.0625/2)*0.0254;       %perimeter
of one cooling channel m
% Al      =   ((0.0625*0.09375)+pi/8*0.0652^2)*0.0254^2;   %area of one
cooling channel m^2
% Dh      =   4*Al/Perl;
% Rel     =   4*(mdotl/Cc)/Perl/mul;
% Prl     =   mul*cpl/kl;
```

```
%%

%Expansion conditions designator (1= equilibrium, 2= frozen);
for eqfz=1:2;

if eqfz == 1    %eq'm
    Kg=1.2633; %W/mk;
    PRg=0.7349;
elseif  eqfz==2
    Kg=1.2102; %W/mk
    PRg=0.7399;
else
    break
end

Tr      =   Tstatic*(1+(gamma-1)/2*PRg^(1/3)*M^2);

%internal convection from Lefebvre:
hg      =   0.017*Kg/(R*2)^0.2*(mg/(pi*R^2*MUG))^0.8;

last = length(S);

%%
for ind=1:length(S)
    qdot1(ind)=1e30;
    qdot2(ind)=1;
    i(ind)=1;
    increment=0.1;
    limit=20000;
    err = 10000;

    Twg(ind)=700;       %guess
    while abs(qdot1(ind)-qdot2(ind))>err && i(ind)<limit
        qdot1(ind)=hg*(Tr-Twg(ind))+0.5*SB*(1+Ew)*Eg*To^1.5*(To^2.5-
Twg(ind)^2.5);
        Ti(ind)=Twg(ind)-qdot1(ind)*ttbc/ktbc;
        Twl(ind)=Ti(ind)-qdot1(ind)*tw/kw;      %backside of Louvre
wall
        %[muwl]= propliq(Twl(ind));
        %Sieder and Tate for large proper variation in turbulent tubes
        %hl(ind)=kl/(4*Al/Perl)*0.027*(Rel)^0.8*Prl^(1/3)*(mul/muwl)^0.
14;
        h2(ind) = 0.020*ka/(Dan^0.2)*(man/(Aan*mua))^0.8;        %from
Lefebvre equation 8-23.
        Rad(ind) = SB*Ew*Ess/(Ew+Ess*(1-Ew));                   %from
Lefebvre equation 8-17.
                                                                %Liner
Emissivity is SS (backside).  Casing Emissivity is TBC
        if ind ==1
            qdot2(ind)=h2(ind)*(Twl(ind)-Ta(ind))+Rad(ind)*(Twl(ind)^4
- Ta(ind)^4);
        else
            qdot2(ind)=h2(ind)*(Twl(ind)-Ta(ind-
1))+Rad(ind)*(Twl(ind)^4 - Ta(ind-1)^4);
```

```
        end
        Twg(ind)=Twg(ind)+increment;
        i(ind)=i(ind)+1;
        error(ind)=abs(qdot1(ind)-qdot2(ind));
    end

    %calculate Tli from Tl-1
    if ind==1
        %do nothing assumed the first point uses the manifold
temperature
    elseif ind == last
        Ta(ind)=Ta(ind-1)+1/(man*cpa)*(X/2)*qdot2(ind)*(2*pi*R);  %72
cooling channels
    else
        Ta(ind)=Ta(ind-1)+1/(man*cpa)*(X)*qdot2(ind)*(2*pi*R);
    end

end
%%

% %determine presure drop
% Pl(1)=413685.44;    %pressure [pa] in manifold 60 psi
% q=(mdotl/Cc)^2/(2*rhol*(Al)^2);
% f=0.0014+0.125/Rel^0.32;
% for ind=2:(last)
%     Pl(ind)=Pl(ind-1)-(4*f*X/(4*Al/Perl)*(q));
% end


%P=P/6894.7573;  %convert pressure to PSI
%q=q/6894.7573;  %convert dynamic pressure to psi
%exporting part ii
% C(1,:)={'Segment','X [m]', 'r [m]','S [m]', 'M', 'P [psi]', 'T [K]'};
% cellwrite('output.txt',C);
% for y=1:length(X)
%     B(y,:)={y,X(y),R(y),S(y),M(y),P(y),T(y)};
% end
% cellwrite('output.txt',B);
%
%Pl=Pl/6894.7573;    %convert liquid pressure drop to PSI
% %exporting2 part iii
% D(1,:)={'Segment','X [m]', 'r [m]','$P_l$ [Pa]',
'$\dot{q}$ [W/$m^2$]','$h_g$ [W/$m^2$K]','$h_l$ [W/$m^2$K]',
'$T_l$ [K]', '$T_{wg}$ [K]'};
% cellwrite('output2.txt',D);
% for y=1:length(X)
%     E(y,:)={y,X(y),R(y),Pl(y),qdot1(y),hg(y),hl(y),Tl(y),Twg(y)};
% end
% cellwrite('output2.txt',E);
%
QDOT(:,eqfz)=qdot1;
HG1(:,eqfz)=hg;
%HL1(:,eqfz)=hl;
TA1(:,eqfz)=Ta;
```

```
TWG(:,eqfz)=Twg;
TWL(:,eqfz)=Twl;
I(:,eqfz)= i;
TI(:,eqfz) = Ti;
ERROR(:,eqfz)=error;
%PL1(:,eqfz)=Pl;
%
end
%
%
% (PL1(1,1)-PL1(last,1))/6894.7573
% (PL1(1,2)-PL1(last,2))/6894.7573
%
%
tplot(1,:)=['equilibrium','frozen'];
 color(1,:)='b- ';
 color(2,:)='r- ';
% color(3,:)='r-.';
% color(4,:)='c--';

% figure(1)
% for v=1:2
%     plot(S,PL1(:,v),color(v,:),'LineWidth',2);
%     hold on;
% end
% legend('Equilibrium','Frozen','Location','Best');
% xlabel('X (m)');
% ylabel('Pl (Pa)');
% grid;

%
figure(2)
for v=1:2
    plot(S,QDOT(:,v),color(v,:),'LineWidth',2);
    hold on;
end
legend('Equilibrium','Frozen','Location','Best');
xlabel('X (m)');
ylabel('qdot (W/m^2)');
grid;
%
% figure(3)
% for v=1:2
%     plot(X,HG1(:,v),color(v,:),'LineWidth',2);
%     hold on;
% end
% legend('Equilibrium','Frozen','Location','Best');
% xlabel('X (m)');
% ylabel('h_g (W/m^2K)');
% grid;
%
% figure(4)
% for v=1:2
%     plot(X,HL1(:,v),color(v,:),'LineWidth',2);
%     hold on;
```

```
% end
% legend('Equilibrium','Frozen','Location','Best');
% xlabel('X (m)');
% ylabel('h_l (W/m^2K)');
% grid;
%
figure(5)
for v=1:2
    plot(S,TA1(:,v),color(v,:),'LineWidth',2);
    hold on;
end
legend('Equilibrium','Frozen','Location','Best');
xlabel('X (m)');
ylabel('T_A (K)');
grid;
%
figure(6)
for v=1:2
    plot(S,TWG(:,v),color(v,:),'LineWidth',2);
    hold on;
end
legend('Equilibrium','Frozen','Location','Best');
xlabel('X (m)');
ylabel('T_{wg} (K)');
grid;

figure(7)
for v=1:2
    plot(S,TWL(:,v),color(v,:),'LineWidth',2);
    hold on;
end
legend('Equilibrium','Frozen','Location','Best');
xlabel('X (m)');
ylabel('T_{wl} (K)');
grid;

figure(8)
for v=1:2
    plot(S,TI(:,v),color(v,:),'LineWidth',2);
    hold on;
end
legend('Equilibrium','Frozen','Location','Best');
xlabel('X (m)');
ylabel('T_{TBC} (K)');
grid;

%
% figure(7)
% plot(X,RHOL)
% xlabel('X (m)');
% ylabel('\rho_l (kg/m^3)');
% grid;
%
% figure(8)
% plot(X,MUL)
```

```
% xlabel('X (m)');
% ylabel('\mu_l (kg/ms)');
% grid;

%subplot(3,2,1)
% figure (3)
%     plot(X,R, 'o');
%     xlabel('X [m]','FontSize',10)
%     ylabel('R [m]','FontSize',10)
%     grid on;
%
% subplot(3,2,2)
%     plot(X,Twg);
%     xlabel('X [m]','FontSize',10)
%     ylabel('Twg [K]','FontSize',10)
%     grid on;
%
% subplot(3,2,3)
%     plot(X,i, 'o')
%     xlabel('X [m]','FontSize',10)
%     ylabel('# of iterations for convergence','FontSize',10)
%     grid on;
%
%     subplot(3,2,4)
%     plot(X,Pl)
%     xlabel('X [m]','FontSize',10)
%     ylabel('Pl [psi]','FontSize',10)
%     grid on;
%
%     subplot(3,2,5)
%     plot(X,M)
%     xlabel('X [m]','FontSize',10)
%     ylabel('M','FontSize',10)
%     grid on;
%
%     subplot(3,2,6)
%     plot(X,Tl)
%     xlabel('X [m]','FontSize',10)
%     ylabel('Tl','FontSize',10)
%     grid on;

   % subplot(3,2,2)
% plot(t,F)
% xlabel('time [s]','FontSize',10)
% ylabel('Thrust [N]','FontSize',10)
% grid on
% subplot(3,2,3)
% plot(t,Cf)
% xlabel('time [s]','FontSize',10)
% ylabel('Cf','FontSize',10)
% grid on
% subplot
```

```
% color(1,:)='b- ';
% color(2,:)='g: ';
% color(3,:)='r-.';
% color(4,:)='c--';
% figure(1)
% for q=1:length(tplot)
%     plot(x,Tw(tind(q),:),color(q,:),'LineWidth',2);
%     hold on;
%     char(q,:)=num2str(tplot(q),'%12.3g');
%     LGD(q,:)=['t=',char(q,:),'s'];
% end
% xlabel('Wall Location (m)');
% ylabel('Temperature (K)');
% legend(LGD);
% grid;
%
% for n=1:length(Tw(:,1))
%     t2(n,1)=t(1,n);
% end
%
% figure(2)
% plot(t2,Tw(:,1));
% xlabel('Time (s)');
% ylabel('Wall Surface Temperature (K)');
% grid;
disp(sprintf('\n Finished.%s\n'));
```